National Technical University of Athens

ALMA MATER STUDIORUM - UNIVERSITÀ
DEGLI STUDI DI BOLOGNA

Master thesis in faculty of nuclear engineering department of university of Bologna and research in Bologna University

Hospital Authority St. Orsola-Malpighi Polyclinic

Design of a low power target for direct cyclotron production of ^{99m}Tc

Presented by:

Anastasia Livanou

Supervisors: *Prof. Ing. Domiziano Mostacci*
Dr. Mario Marengo

Correlator: *Prof. Marios Anagnostakis*

This page was intentionally left blank

1. Executive Summary

The basis of this thesis is the design and construction of a target support capable to host a variety of materials (pellets, metal foils, etc.) for cyclotron production of 99mTc in quantities sufficient for local clinical use without requiring complicated and expensive techniques of target preparation.

The need to conduct this thesis emerged due to shortages of reactor produced 99Mo-99mTc leading to the alternative direct production of 99mTc via the 100Mo (p,2n)99mTc reaction in the cyclotron.

In this thesis, which was conducted at the Medical Physics Unit of the Bologna Hospital ‘’S.Orsola-Malpighi University Hospital‘’ I designed an optimized target disc for the GE PETrace cyclotron using Solidworks software. In particular, Solidworks was chosen because it’s ideal when creating a full solid model in a simulated environment for both design and analysis.

The new target system was made of two parts: a support (or backing) intended to contain the effective target material, and a front piece that keeps the target material in position. Copper was selected as the material of choice, due to its availability, relatively low cost, excellent thermal conductivity, and ease of machining.

For the design verification and validation, a testing plan was created which incorporated specifications of the applicable operational parameters as well as the acceptable performance criteria.

By reviewing the usage of a very similar existing technological solution, it has been concluded that practically no structural stress is applied to any of the parts of the apparatus, either during the initial fitting, or during the radiation bombardment.

Thermal simulations were performed using Ansys Software, and the results showed that the temperatures near the target face – the area most exposed to heat stress - remained well below the material melting temperature (copper melting temperature-1082,3 oC) which ensured the physical integrity of the target disc.

Due to time limitations, only limited testing of the first prototype of the target support was possible.

The enriched target material used was a series of 5 100Mo sheets. The target was irradiated for 90 minutes at a current of 20 μA. A final solution of purified 99mTc pertechnetate was obtained, with an activity of 686 MBq at 4h. A sample of 259 MBq was taken from the final solution and injected into a typical phantom for evaluation of the performance in SPECT imaging, and a tomographic acquisition was performed using a Siemens E.cam dual head gamma camera, fitted with Low Energy High resolution collimators. Tomographic acquisition was also performed.

In conclusion, this work successfully represented a first step in a new direction of investigation into the design of a new low power target for cyclotron production of 99mTc.

Table of Contents

Table of Figures

2. Introduction

2.1.1 This thesis is consisted of:

- the theoretical part which involved literature review
- the experimental part which was performed at the Medical Physics Unit of the Bologna Hospital ‘’ S. Orsola-Malpighi University Hospital ‘’

2.1.2 The basis of this thesis is the design and construction of a target support capable of hosting a variety of materials (pellets, metal foils, etc.) for cyclotron production of ^{99m}Tc in quantities sufficient for local clinical use without requiring complicated and expensive target preparation techniques.

2.1.3 The need to conduct this thesis emerged due to shortages of reactor produced ^{99}Mo-^{99m}Tc leading to the alternative direct production of ^{99m}Tc via the ^{100}Mo (p,2n)^{99m}Tc reaction in the cyclotron.

2.1.4 Technetium-99m (^{99m}Tc) is the most widely used radioisotope in nuclear medicine today, and accounts for over 80% of the present 3.2 billion dollar global market in radiopharmaceuticals.

2.1.5 It is favoured due to its single 140 keV emission during decay, its short half-life of 6 hrs that minimize patient’s dose during imaging, and its normal production route whereby its ^{99}Mo precursor is distributed to hospitals in a generator which is then eluted to obtain the ^{99m}Tc built up from the ^{99}Mo decay.

2.1.6 ^{99}Mo is today primarily obtained via fission of HEU targets, each irradiated for several days in one of several ageing research reactors. A crisis is looming due to the shutdown of one of the largest production facilities at Chalk River in Canada in 2016.

2.1.7 The purpose of this work is to design, fabricate and test a mechanism that would make the production of the PET isotope, ^{99m}Tc practical for both researchers and commercial suppliers. The planned outcome of this project was the development of ^{99m}Tc production method using the reaction of ^{100}Mo (p,2n)^{99m}Tc in cyclotron .

2.1.8 The design could be optimized if future isotope demand exceeded current requirements.

3. Thesis structure

3.1.1 Chapter 1 describes summarily the production of radionuclides by conventional methods (cyclotron, reactor). It also describes radionuclides used for imaging.

3.1.2 Chapter 2 presents a full description of the GE PETtrace cyclotron, installed at “S. Orsola-Malpighi” Hospital (Bologna, IT) and its subsystems.

3.1.3 Chapter 3 is devoted to direct production of 99mTc as an alternative to traditional methods.

3.1.4 Chapter 4 describes the design development of a simple low power target disc for irradiation of pellets.

3.1.5 Chapter 5 describes the thermal simulation parameters / characteristics and presents the simulation outputs. Discussion of the results is also contained in this chapter.

3.1.6 Chapter 6 describes the initial irradiation test using the prototype designed.

3.1.7 Finally, conclusions and hypothesis of future work are provided in conclusion.

4. Background

4.1.1 Particle accelerators were initially developed to address specific scientific research goals, yet they were used for practical applications, particularly medical applications, within a few years of their invention.

4.1.2 From its inception in 1930 by Ernest Orlando Lawrence, and throughout its many design variations to increase particle energy and intensity for research, the cyclotron has been used for a variety of biological, medical and industrial applications.

4.1.3 Soon after the first experimental demonstration of the cyclotron resonance principle by Earnest Lawrence and Stanley Livingston, new radioisotopes produced by high energy particles were discovered and used for the study of both biological processes and chemical reactions.

4.1.4 The cyclotron's potential for producing beams for cancer therapy and medical radioisotope production was realized with the early Lawrence cyclotrons and has continued to grow with more technically advanced successors: synchrocyclotrons, sector-focused cyclotrons and superconducting cyclotrons. These medical and industrial applications eventually led to the commercial manufacture of both small and large cyclotrons and facilities specifically designed for applications other than scientific research.

4.1.5 The building of the cyclotron made possible the routine production of radionuclides that would find use in a variety of applications, including medicine, industry, agriculture, and basic physical and biological research. With the high power of the charged particles (energy and flux or beam current) available in the cyclotron, it is possible to produce abundant quantities of a wide variety of radionuclides.

4.1.6 In the medical field, cyclotrons are used both in diagnosis and therapy. In diagnosis they are used in the production of radioactive isotopes. In particular, in the tracers for Positron Emission Tomography (PET).

4.1.7 The positron emission tomography (PET) has an important role in diagnostic imaging. The standard radionuclides used in PET imaging are produced by cyclotron irradiation of liquid or gaseous targets and are used for the detection and staging of various tumours, etc.

4.1.8 The fragility of 99Mo supply has recently come to light during recent shutdowns of reactors which are typically more than 40 years old and are at risk of prolonged or permanent shutdown in the near future, creating a risk for loss of a long-term, stable supply of 99Mo for medical purposes.

4.1.9 Much research work is in progress on the study of alternative methods for the production of 99mTc in quantities and with the degree of purity required for clinical use.

4.1.10 The cyclotron option could be viable for a number of reasons.

- First, cyclotrons are widely diffused and established in industrial facilities, hospitals and research sites, a fact that makes it an easily testable option with minimal cost.
- Second, with successful process demonstration and target development, this option is scalable and the cyclotrons may be used as multi-use facilities since they are primarily qualified for producing PET and other isotopes.

4.1.11 Finally, communication and collaboration between medical cyclotron operators could ensure redundancy in supply and avoid single point of failure in the supply chain.

5. Chapter 1 Production of radionuclides

5.1.1 The development of nuclear technology was one of the most significant achievements of the twentieth century.

5.1.2 The unique properties of radionuclides have led to numerous applications in pure and applied scientific research, medicine, and industry. Nuclear medicine relies on the decay of radioisotopes for the diagnosis and treatment of diseases. In nuclear medicine procedures, radionuclides are made into compounds to form radiopharmaceuticals that can have localized effect on specific organs or cells. In industry and in other scientific research, radioisotopes are primarily used as tracers to monitor processes and as probes to measure the magnetic and electric fields in condensed matter. [1]

5.1.3 The pioneering work of Marie and Pierre Curie in uncovering substances with previously unrecognized properties, for which they coined the term radioactive, opened up many new fields of opportunity. The Curies' discovery was the result of Marie Curie's belief that the ore pitchblende contained another, more active, substance than uranium. Within a few months of starting to analyze pitchblende in 1898, Marie Curie had isolated two previously unknown elements. She named the first polonium, after her native Poland; the second she called radium, in response to its intense radioactivity. Practical applications in scientific research for radioisotopes followed from these discoveries in the period from 1920 to the early 1930s. However, the few naturally occurring radioisotopes that were available severely limited the scope of what was possible. The full potential was not realized until radioisotopes could be produced artificially. After the War the wide use of radioactive materials in medicine established the new field of what was then called atomic medicine, which later became known as nuclear medicine. Radioactive carbon, tritium, iodine, iron, and chromium began to be used more widely in the study of disease processes.

5.1.4 Nuclear medicine has its origins in the pioneering work of the Hungarian physician George de Hevesy, who, in 1924, used radioactive isotopes of lead as tracers in bone studies. Shortly thereafter, R. H. Stevens made intravenous injections of radium chloride to study malignant lymphomas .As indicated below, the first medical cyclotron was installed in 1941 at Washington University, St. Louis, where radioactive isotopes of phosphorus, iron, arsenic and sulfur were produced. With the development of the fission process during the Second World War, most radioisotopes of medical interest began to be produced in nuclear reactors.

5.1.5 Ben Cassen , in 1951, developed the concept of the rectilinear scanner, which opened the way to obtaining in a short amount of time the distribution of radioactivity in a subject. This was followed by production of the first gamma camera by Hal Anger in 1958. The original design was modified in the late 1950s to what is now known as the anger scintillation camera, thus heralding the modern era of gamma cameras, whose principles are still in use today. Powell Richards developed the 99Mo/99mTc generator system at Brookhaven National Laboratory in 1957. Technetium-99m produced via this generator system has become the most widely used radionuclide in nuclear medicine today, accounting for as many as 85% of all diagnostic procedures.[2]

5.1.6 Diagnostic nuclear medicine makes use of the fact that certain radioisotopes emit gamma rays with sufficient energy that the gamma rays can be detected outside of the body. If these radioisotopes are attached to biologically active molecules, the resulting compounds are called radiopharmaceuticals. They can either localize in certain body tissues or follow a particular biochemical pathway.

5.1.7 Today, the majority of radionuclides are artificially produced in the cyclotron and reactor. Some short-lived radionuclides are available from the so-called radionuclide generators in which long-lived parents are loaded and decay to short-lived daughters.[2]

5.2.1 The transformation of one element into another was first demonstrated by Ernest Rutherford in 1919, when he directed the α particles emanating from a sample of polonium onto nitrogen gas and detected the protons being emitted (having produced O-17). The future of accelerator production of radioisotopes reached a turning point with the construction of the cyclotron by Ernest Lawrence in 1931 and has been developed over the last 8 decades into machines that can provide any ion and energy desired for research or applications given the practical limit of cost .The applications of cyclotron beams in medicine and industry have grown from the first investigations of Lawrence's brothers in the 1930s to the point where commercial cyclotrons are designed and built to specifications to meet a large array of user applications, including industry, national security and medicine. [3]

Figure 1. The Lawrence brothers at the console of the first cyclotron used for isotope production and radiation treatments with neutron beams.

5.2.2 Cyclotrons are particle accelerators that use a fixed magnetic field to constrain charged particles to nearly circular orbits that are synchronous with a radio frequency (RF) accelerating field. The charged particles repeatedly traverse the electric field produced by the RF electrodes, increasing in energy at each traversal. That is to say, the charged particle's period of revolution in the fixed magnetic field of the cyclotron is independent of the particle's momentum. [4]

5.2.3 In the field of medicine their use is both in diagnosis and therapy. In vivo diagnostic studies are performed using suitable radionuclides, i.e. pure gamma emitters or positron emitters. Whereas the former are produced using both nuclear reactors

and cyclotrons, the latter, being neutron deficient, can be produced only at a cyclotron via charged-particle-induced reactions. With the cyclotron, it became possible to produce radioactive isotopes of a wide variety for the first time.

5.2.4 Cyclotrons have become the tool of choice for producing the short-lived, proton rich radioisotopes used in biomedical applications.[5,6] Cyclotron produced medical isotopes are used in planar (2D) imaging studies with the gamma cameras, and tomographic studies (3D) such as Single Photon Emission Computed Tomography (SPECT) and Positron Emission Tomography (PET). Generally a compound labeled with a radioactive tracer, prepared in a modular chemistry unit from an irradiated target material, is introduced in vivo. The tracer element, a gamma emitter or positron emitter, travels through the body and accumulates in specific parts or tissues of the body depending upon the chemistry of the compound, which can then be imaged for clinical diagnostic purposes or treatment. The use and need of radioactive isotopes for biomedical applications continues to increase worldwide. [7]

5.3.1 Immediately after World War II, almost all radionuclides and radioisotopes in use were made in a reactor. The first operating nuclear reactor that used natural uranium as fuel and graphite blocks as moderator (graphite reactor) was constructed in Oak Ridge, Tennessee, USA and operated from 1943 to 1963. 8 From 1950 to 1970 a large number of research reactors with multiple facilities were constructed. After 1980, because of the decommissioning of many old ones, the number of operating reactors has been steadily decreasing.

5.3.2 A nuclear reactor is constructed with fuel rods made of fissile materials such as enriched ^{235}U and ^{239}Pu.These fuel nuclei undergo spontaneous fission with extremely low probability. Fission is defined as the breakup of a heavy nucleus into two fragments of approximately equal mass, accompanied by the emission of two to three neutrons with mean energies of about 1.5MeV. Radioisotopes are produced by exposing suitable target materials to the neutron flux in a nuclear reactor for an appropriate time. Target materials to be irradiated are sealed in primary capsules, loaded in specially designed irradiation jigs and then lowered in predetermined locations in the core for irradiation. The irradiated targets are then loaded in appropriate shielding containers and transported to the radioisotope processing laboratories.

5.4.1 Nuclear medicine imaging differs from other types of radiological imaging, in that the radiotracers used in nuclear medicine map out the function of an organ system or metabolic pathway and, through the imaging the concentration of these agents in the body the integrity of these systems or pathways is revealed. This is the basis for the unique information that a nuclear medicine scan provides with various scanning procedures for the various organ/functional systems of the body.

5.4.2 The list below, provides the various low energy production routes along with the half-lives of the radioisotopes. Technetium-99m is included, since this isotope alone accounts for nearly 85% of all nuclear medicine imaging prospect for producing Mo-99 or Tc-99m directly via charged particle reactions or from photons needs to be revisited.

Radionuclide	*t*1/2	Reaction	Energy (MeV)
99mTc	6.0h	^{100}Mo(*p,*2*n*)	30
123I	13.1h	124Xe(*p,*2*n*)123Cs	27
		124Xe(*p,pn*)123Xe 124Xe(*p,*2*pn*)123I 123Te(*p,n*)123I	 15
		124Te(*p,*2*n*)123I	25
201Tl 11C	73.1h 20.3m	203Tl(*p,*3*n*)201Pb→201Tl ^{14}N(*p,α*)	29 11–19
		^{11}B(*p,n*)	10
18F	110m	^{18}O(*p,n*)	15
		^{20}Ne(d,*α*)	14
		^{nat}Ne(*p,X*)	40
64Cu	12.7h	^{64}Ni(*p,n*)	15
		^{68}Zn(*p,αn*)	30

		^{nat}Zn(*d,αxn*)	19
		^{nat}Zn(*d,*2*pxn*)	19
124I	4.14d	^{124}Te(*p,n*)	13
		^{125}Te(*p,*2*n*)	25

Table 1. The most widely used radionuclides for imaging, along with a couple of potentially useful radionuclides.

5.4.3 Pet imaging has been in use for several decades for human brain and whole body imaging, first only as a research tool, now gaining acceptance as a diagnostic imaging modality in selected applications such as oncology and, very recently, as an aid in the diagnosis of Alzheimer's disease. All of these advances have been made possible through the improvement in resolution and sensitivity of the scanners but, more importantly, through the development of more specific tracers.

6. Chapter 2 GE PETtrace Cyclotron

6.1 The GE PETtrace Cyclotron

6.1.1 The cyclotron used in the experimental tests and to which simulations set-up refers, was a PETtrace (GE Medical System), a compact cyclotron with vertical acceleration plane, capable of accelerating negative hydrogen H- and deuterium D- ions up to an energy of 16.5 and 8.4 MeV respectively, designed for the fast, easy, and efficient production of PET radiotracers. Maximum beam intensity of 100 μA and 60 μA can be achieved (after a recent hardware upgrade) for hydrogen and deuterium ions respectively. The cyclotron is installed and used in the S. Orsola-Malpighi University Hospital (Bologna, IT) for the routine production of PET radionuclides.

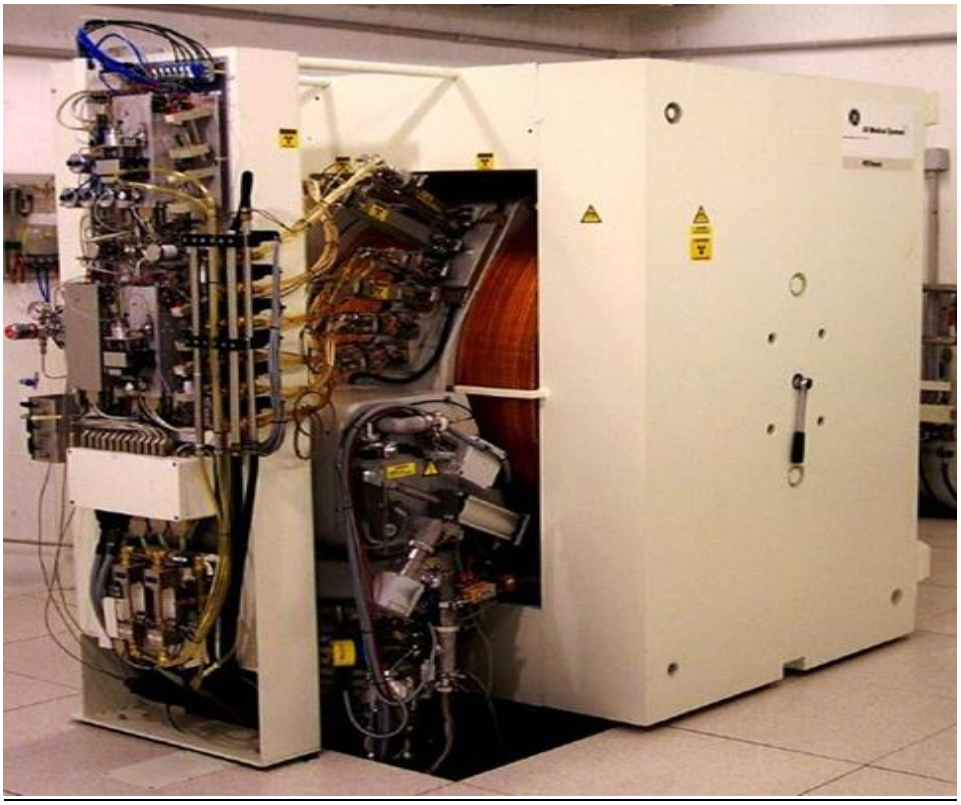

Figure 2. The GE PETtrace cyclotron installed at "S. Orsola-Malpighi" Hospital.

6.1.2 It consists of a large cylindrical chamber, placed between the poles of a huge electromagnet and used for accelerating the charged particles. The chamber is exhausted until a very high vacuum exists inside. Negative hydrogen H- and deuterium D- ions, used as bullets, are fed into the center of the chamber by means of an ion source. Inside the chamber are two hollow, D-shaped electrodes, called Dees, which are connected to a source of very high voltage, oscillating with high frequency (RF).When the cyclotron is in operation, the electric charge on these Dees is reversed very rapidly, due to the high frequency voltage. The combination of the high voltage alternating potential and the action of the field of the electromagnet causes the H– or D– ions inside to take a spiral course. They move faster and faster and acquire more and more energy. When they reach the outer rim of the chamber, the H– or D– ions are transformed to protons or deuterons and then deflected toward a target (the PETtrace has up to six targets). As the target is hit by this beam of high energy particles, the appropriate target

liquid or target gas is transformed into a short half-life radioactive substance, emitting positrons—a so called PET tracer. As a matter of fact, the beam of accelerated particles can be directed on one of the 6 output ports available. The cyclotron is equipped with several target assembly, the components in which nuclear reactions happen. Multiple thin “stripper foils” can be inserted at several radii within the cyclotron, making it possible to simultaneously extract several H+ beams of different energies from a single cyclotron. The energies that are obtained are used to create the commonly used PET radioisotopes such as ^{11}C, ^{13}N, $^{18}F^-$, $^{18}F_2$ and ^{64}Cu. The cyclotron is able to operate in a dual beam condition, i.e. two target assembly can be irradiated at the same time.

6.1.3 In the following, details of the different cyclotron subsystems will be. The PETtrace can be divided into several subsystems:

- Magnets
- Source of radio-frequency
- Ion source
- Extraction system of the beam
- Control system of the beam
- Vacuum system
- Targets.

6.2 The magnets

6.2.1 The bearing structure of the magnets is of standard industrial steel with low content of carbon (<0.18%); the poles of the magnet, that are also of steel with a low carbon content (<0.05%), are a single piece forged. The poles of the magnet are divided into two different areas, the hills and valleys (the valleys are created by removing radial sectors of the magnet), as can be seen in Figure 3. The magnetic field is induced by copper hollow conductors inside which circulates demineralized water for refrigeration. The magnet is oriented vertically.

Figure 3. Ge PETtracer magnets.

6.3 The source of radio-frequency

6.3.1 The particles are accelerated by the radiofrequency system that is connected to two of the 4 dees present, which are placed at an angle of 75º; the other two dees are connected to the ground. The negative hydrogen ions are accelerated in the first harmonic in order to be accelerated to 4 times for each revolution, while the deuterium ions are accelerated in the second harmonic and get two accelerations for each revolution. The mass difference between the two types of particles that the cyclotron is capable of accelerating, in addition to affect the intensity of the magnetic field to be applied, determines a different choice of the frequency of oscillation (27.2 MHz for H− ions, 27.8 MHz for D− ions), that are generated by the RFPG (Radio Frequence Power Generator, placed outside the bunker in which the cyclotron is installed) connected to the electrodes via a coaxial cable (RF Feeder Cable) which transmits radio-frequency.

6.4 The ion source

6.4.1 The ion source is located in the center of the cyclotron and it is a cold-cathode-type PIG (Penning ion gauge) source. The ion source contains in its interior two separate chimneys, one for the production of H− and the other for the D−. The method with which the ions are produced is the same for the two types of particles. Inside a cylindrical chamber there is the electrical discharge produced by a huge electric tension applied between the anode (side surface of the cylinder), connected to the ground, and two cathodes (bases of the cylinder), to which is applied a negative voltage generated by the PSARC (Power Supply Ion Source). The plasma of ions and electrons which is created remains confined inside the chamber for the presence of the magnetic field. On one side of the chamber there is a small slit. The ions H− and D− come out from the chamber when a positive voltage is applied to the dee which is located close to the slit. The slits for the two types of particles are located at opposite positions. The H− are extracted from the dee mounted in the lower part of the cyclotron, while the D− are extracted in the upper part.

6.5 The extraction of the beam

6.5.1 The extraction of the beam is based on the technique of the stripping foil. The two electrons of the H− and D− ions are stripped during the passage of the beam through a thin foil of carbon (3 μm thick). The charge of the accelerated particles changes from negative to positive, involving a change of the direction of rotation of the beam. The electrons collected by the foil allow a constant monitoring of the beam current. The PETtrace is equipped with two extraction units each of which can extract the beam to three of the six output ports. The extraction units slide on a curved track mounted along the radius of extraction. Each unit contains 6 carbon foils mounted on a revolver which, rotating on itself, is able to change the carbon foil when this is damaged. Having two extraction units allows the PETtrace to operate in dual beam (it is possible to irradiate two targets simultaneously). The technique of stripping foil allows an efficiency of extraction of the beam equal to 100%.

6.6 The control system of the beam

6.6.1 The cyclotron is provided with various monitoring systems of the beam current, both in the vacuum chamber and on the targets. The system includes a retractable probe positioned at a small radius of the orbit of acceleration, the stripping foil, two collimators and the body of the target. All these systems are isolated from the ground to allow a correct measure of current. The tantalum probe is located in the proximity of the ion source and it is used at the beginning of irradiation to set the optimal current for the production of the radioisotope. A correct reading of the current in this phase of irradiation allows to control that the accelerator and the various subsystems are functioning properly. The foils, in addition to changing the direction of rotation, allow a constant monitoring of the beam intensity, measuring the current created by the electrons extracted from the negative accelerated ions. The collimators are placed on the inner part of the output ports. They are also in tantalum or graphite and are used to center the beam, cutting each non-aligned

tail. Also the body of the target is isolated from the ground to allow the measure of the effective current present on the target material during the production of radioisotopes. All the signals useful for the monitoring of the beam are connected to the multichannel BCA (Current Beam Analyzer).

6.7 The vacuum system

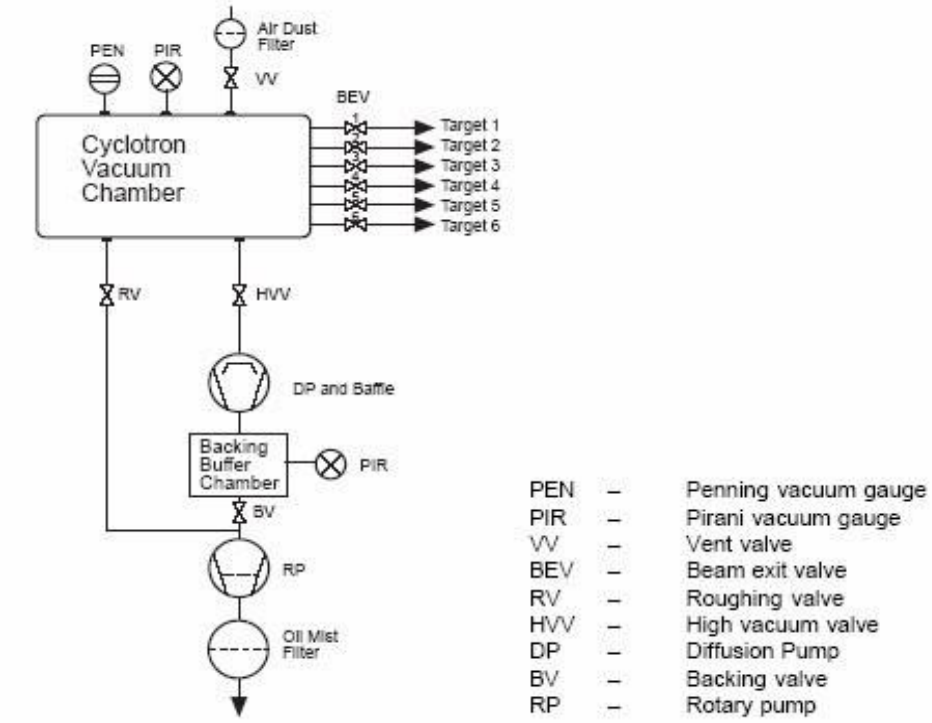

Figure 4. Diagram of the system to produce the vacuum.

6.7.1 Since the binding energy of the second electron in a hydrogen atom is very low (0.755 eV), it is therefore essential, in order to accelerate negative ions, to create highvacuum inside the cyclotron, about an order of magnitude more than in a cyclotron that accelerates positive ions . The vacuum is made with the aid of two pumps, a rotary pump to generate the pre-vacuum and a diffusion pump to bring the vacuum inside the chamber in optimum working conditions. The pumps are connected to the acceleration chamber of the cyclotron through a high-vacuum valve. To measure the wide range of pressure inside the vacuum chamber are installed two pressure switches: the Pirani pressure switch, capable of measuring pressures from 1 bar to 103 mbar and the Penning pressure switch for the measurement of high vacuum (< 103 mbar).

Constant pressure without gas flow (pressure reached after 48 h)	$5 \times 10^{-7} \pm 2 \times 10^{-7}$ mbar
Pressure reached after 1 h	6×10^{-6} mbar

($P_{t=0}$ = 1 atm)	
Pressure during irradiation (φ = 5 sccm/min)	4 ×10^{-5} mbar
Pump capacity	2600 l/s

Table 2 . Specifications in normal working conditions.

6.7.2 The vacuum system is fully automated and controlled by the VCU (Vacuum Control Units), that constantly works.

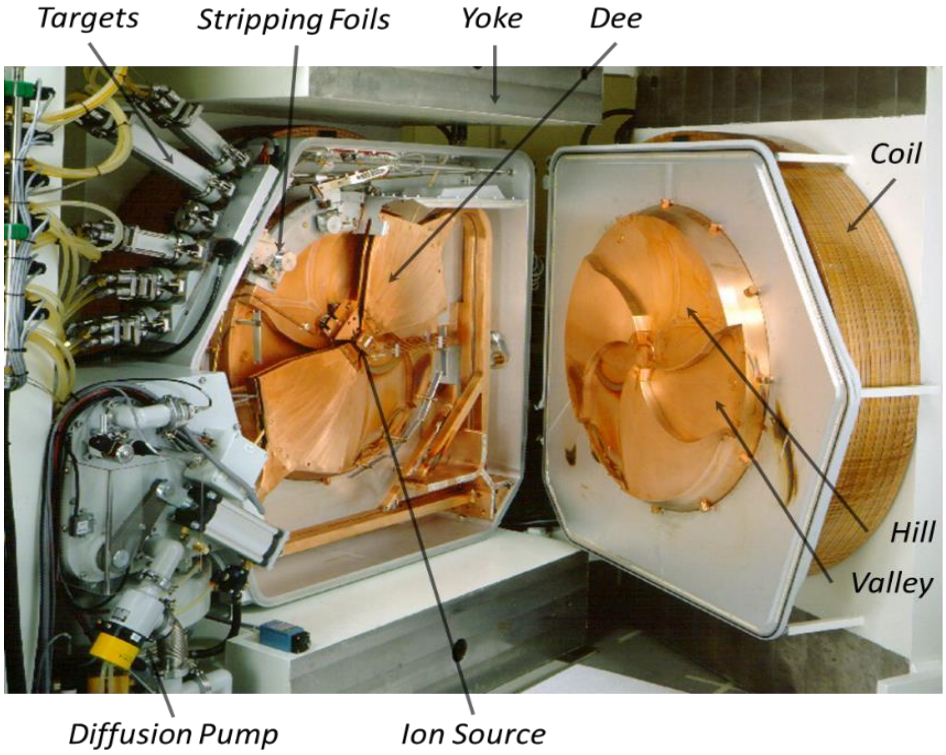

Figure 5 . Overview of the vacuum chamber and the main components of the GE PETtrace cyclotron.

6.8 The targets

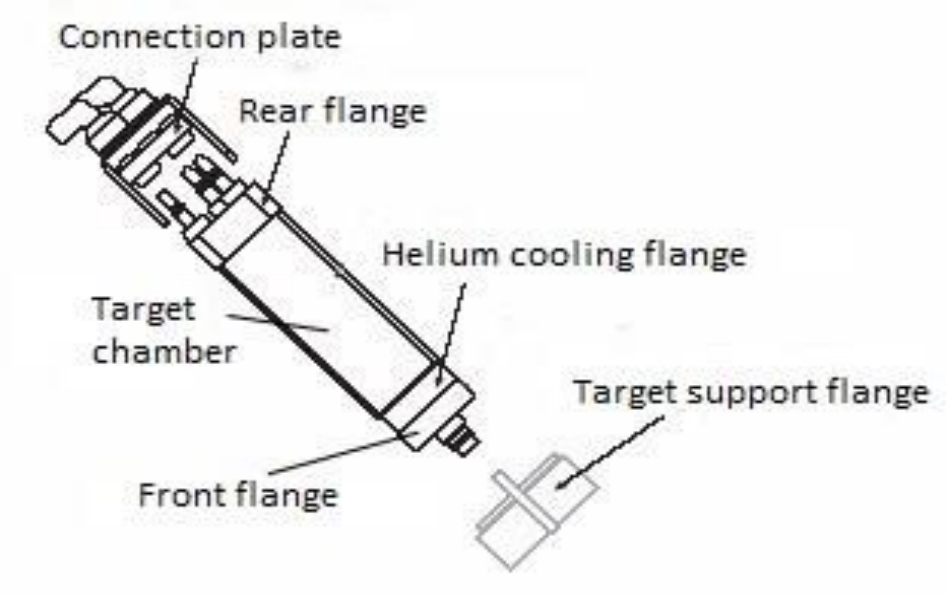

Figure 6 . Structure of a generic target.

6.8.1 When the particle beam has passed the selected extraction foil, it hits the corresponding target at the cyclotron beam exit. The targets, in terms of the total assembly, are mounted on a flange at the front of the cyclotron. The particle beam hits and transfers its energy to the target material and thus the nuclear reactions (required for the radionuclides production) take place. In the standard configuration, the cyclotron has six beam exit ports.

6.8.2 Each beam exit is equipped with a vacuum gate valve (Beam Exit Valve or BEV) and a conical fitting for the target body. The target is locked into position by quick connections. All external connections to the targets, target pressure transducers and liquid target fillers (LTF) are located at the Target Panel. The Target Panel is mounted in front of the cyclotron, close to the targets. The Helium Cooling System is a closed system, which facilitates cooling of the target foils.

6.8.3 The system includes the piping and valves for gas distribution, a heat exchanger, and a compressor for high-speed recirculation of the helium gas.

6.8.4 Each target consists of a front flange for the connection to the cyclotron, a Helium cooling flange, a chamber where the target material is placed and a rear flange for connection to the different cooling and sorting supports. The front flange guides the target in the correct mounting position; all the targets can be easily installed and removed with a lever, which simplifies operations. The target chamber is separated from the vacuum chamber of the cyclotron by two thin HavarTM foils (42.5% Co, 20% Cr, 17.86% Fe, 13% Ni, 2.8% W, 2% Mo, 1.6% Mn, 0.2% C, 0.04% Be), a non-magnetic resistant alloy.

6.8.5 During the irradiation, helium circulates between the two HavarTM foils at a pressure of about 0.5 MPa, which allows the cooling of the metallic foils. The

target material can be liquid, gaseous or solid depending on the nuclide to produce.

6.8.6 The design and the type of material used for the construction of various targets is made in order to dissipate the heat developed by the interactions, to withstand the intense radiation beam to which the whole body of the target is subjected and especially to maximize the nuclear reaction of interest.

6.8.7 The aluminum is chosen due to the excellent properties of activation of the metal, in fact, the activation products have a short half-life and are relatively few compared to those generated in alternative metals. The aluminum has a good ductility and a high thermal conductivity (247 W K m-1).

6.8.8 All target supports (target material, water to cool the body of the target, helium for the cooling of the metallic foils) enter and leave the target through the rear flange. Because the target is made up of several pieces assembled together it is crucial to ensure an adequate sealing.

6.8.9 The seal is obtained by interposing O-rings of plastic material, such as Viton, or metal (Helicoflex) between the surfaces. The GE PETtrace installed at “S. Orsola-Malpighi” University Hospital is equipped with an experimental solid target station, developed locally (Cicoria, et al., 2006).

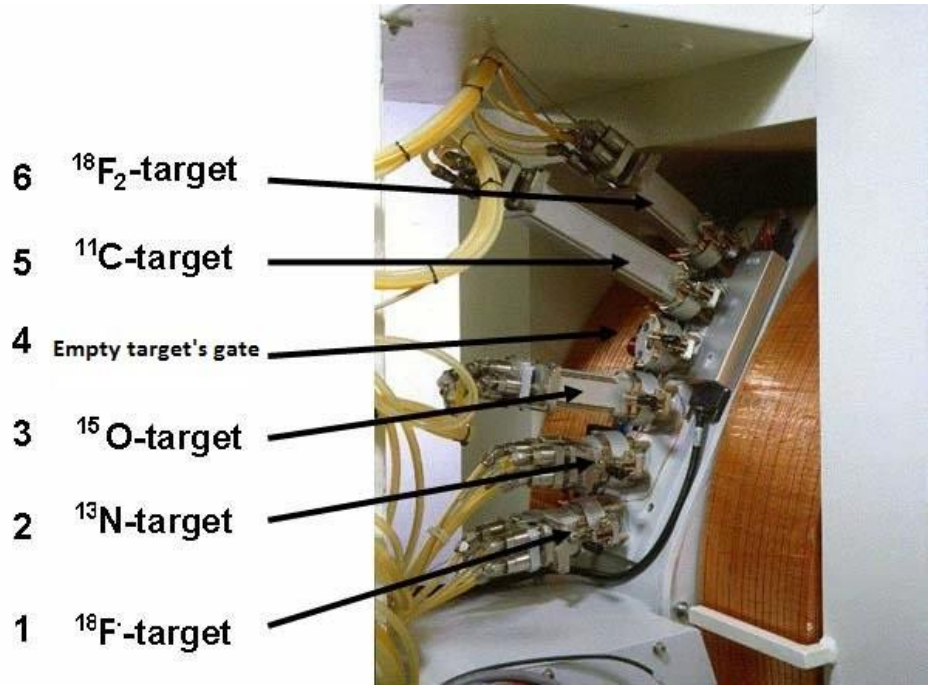

Figure 7 . Targets installed on the GE PETtrace.

6.8.10 The Secondary Water Cooling System provides a closed loop with deionized cooling water for the Cyclotron subsystems.

6.8.11 This system consists of the Secondary Water Cooling Unit, which continuously deionizes the water, and two water manifolds that distribute the cooling water. A primary system for the cooling of the Secondary Cooling Unit must be provided by the customer.

6.8.12 The Primary Cooling System can consist of a water cooling tower or a refrigeration system. There should be a temperature regulation system in the Primary Cooling

System to control the temperature of the Secondary Cooling System. Start-up and shutdown of the Secondary Water Cooling System is done automatically by the Control System. Flow switches in all of the secondary circuits provide interlock signals to the ACU.

6.8.13 The Mains Distribution Panel (MDP) handles the distribution of mains power to PETtrace subsystems, including the Power Distribution Unit. The Power Distribution Unit (PDU) handles the distribution of mains power to subsystems as the Vacuum

6.8.14 System, the Helium Compressor (Target System), the Magnet door and others. The Accelerator electronics and power supplies are housed in equipment cabinets placed in the technical room outside the cyclotron vault.

6.8.15 The PETtrace system is computer-controlled. The Control System comprises four primary units:

- Master System exercises operational control over the tracer production runs and provides the primary interface between the PETtrace system and its operator.
- Accelerator Control Unit (ACU) provides the control interface between the Master System and the Accelerator.
- Chemistry Control System (CCS) provides the control interface between the Master System and the Radiochemistry System.
- PETtrace Service System (PSS) provides a dedicated maintenance terminal for system service.

Target	Target material	Nuclear reaction	T (min)	Chemical form
^{15}O	N_2 (gas)	$^{14}N(d,n)^{15}O$	2	^{15}O-O_2
^{13}N	H_2O (liquid)	$^{16}O(p,\alpha)^{13}N$	10	^{13}N-NO_x
^{11}C	N_2+1% O_2 (gas)	$^{14}N(p,\alpha)^{11}C$	20	^{11}C-CO_2
^{18}F-F–	$H^{18}{}_2O$ (liquid)	$^{18}O(p,n)^{18}F$	110	^{18}F-F–
^{18}F-F_2	^{20}Ne+1% F_2 (gas)	$^{20}Ne(d,\alpha)^{18}F$	110	^{18}F-F_2

Table 3 . Main features of the radionuclides produced routinely and for research purpose at “S. OrsolaMalpighi” Hospital.

7. Chapter 3 Direct production of 99mTc as an alternative to traditional methods

7.1.1 Technetium- 99m (^{99m}Tc) continues to be the most widely utilized radioisotope in nuclear medical imaging today, with more than 85% of administered radiopharmaceuticals being produced[10] by this isotope and global consumption exceeding 40 million scans per year[11]. Since 1937, when Carlo Perrier and Emilio Segrè discovered the element of atomic number 43, isolated by deuteron bombardment of molybdenum, ^{99m}Tc has evolved as the most widely used radioisotope in nuclear medicine. The name technetium was coined from Greek to denote that this was the first artificial element made by man, and the chemical symbol was suggested to be Tc.[12]

7.1.2 Since the selection of ^{99m}Tc as the radionuclide of choice for diagnostic imaging, there has been an ever-increasing demand and it has evolved as the most commonly used medical isotope. It is estimated that every year 30 million patients undergo ^{99m}Tc procedures around the world .13A variety of -labelled radiopharmaceuticals are now used daily in about 70,000 medical imaging procedures worldwide.[14]It's versatile and can be used to produce some 20 different compounds for the detection of disease and for the study of organ structure and function. It's especially useful for nuclear medicine procedures because it can be injected into the body, chemically incorporated into small molecule ligands and proteins and concentrate in specific organs or tissues in order to verify their function.

7.1.3 Consequently, the preeminence of ^{99m}Tc is also attributable to the low dose required for medical imaging, its optimal nuclear properties of half-life of only six hours (which ensures that it does not remain in the body very long) and a gamma photon emission of 140 keV, which is suitable for high-efficiency detection and results in low radiation exposure to the patient.

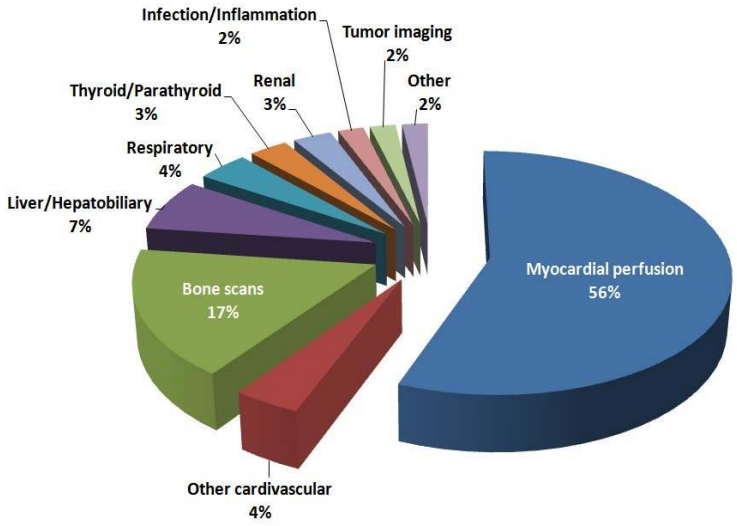

Sources: IMV 2007 Nuclear Medicine Market Summary Report, October 2007, Burns 2007, SECOR Analysis

Figure 8 .The types of nuclear medicine procedures that can be done using Tc-99m

7.1.4 ^{99m}Tc is obtained from the decay of its parent isotope Molybdenum-99 which is a radioactive isotope that undergoes beta decay with about a 66 hour half-life (Fig. 4.2). About 88% of these decays result in the production of the metastable isotope 99mTc, which subsequently decays to the ground state (^{99g}Tc) with about a 6 hour half-life. The present process for producing ^{99}Mo for medical isotope use involves the neutron fission of ^{235}U (i.e. ^{235}U (n,f)^{99}Mo) (Figure 9). About 6.1% of the ^{235}U fissions produce ^{99} Mo. The cross-section for this reaction is large (~584 barns for thermal neutrons) compared with other production processes. Multipurpose research reactors are especially well suited for 99Mo production because they have space for irradiating multiple targets at high neutron fluency rates (typically in the order of 1013–1014 neutrons per square centimeter per second (n·cm–2·s–1][15]

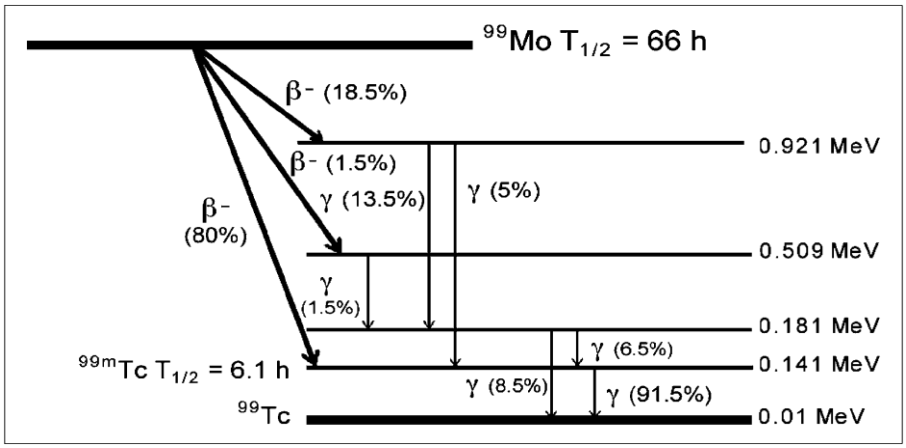

Figure 9 . ^{99}Mo decay.

7.1.5 Molybdenum-99 can be produced through a number of other schemes illustrated in Figure 10:

- Fission of ^{235}U with neutrons produced in deuteron and proton accelerators through (D, n) and (p, n) reactions on heavy targets.
- Neutron activation of ^{98}Mo (i.e. ^{98}Mo (n, γ) ^{99}Mo). This process is only practical for reactor based production owing to the small activation cross-section (0.13 b for thermal neutrons). Also, 99Mo produced through this process has a lower specific activity than neutron fission produced ^{99}Mo.
- Photofission of ^{100}Mo (i.e. ^{100}Mo (γ, n)^{99} Mo). The energetic photons used in this production scheme are obtained by irradiating heavy targets with electron beams produced by linear accelerators.

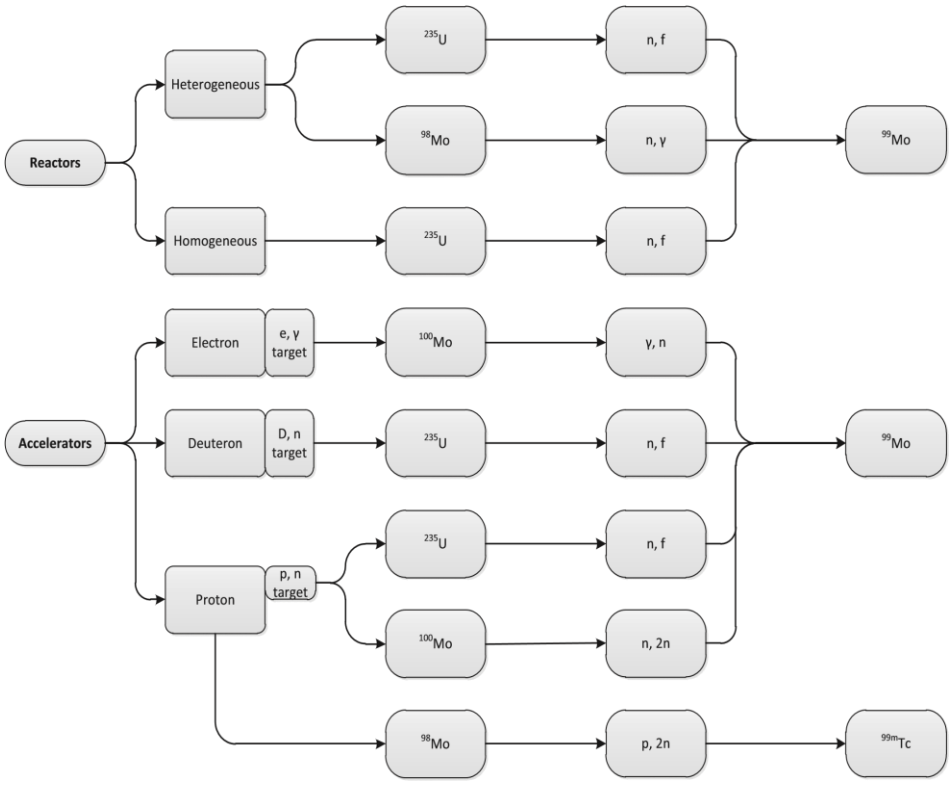

Figure 10. Schemes for producing 99Mo and 99mTc

7.1.6 At present, most of the world's supply of ^{99}Mo for medical diagnostic imaging is produced by irradiating solid targets containing ^{235}U in Belgium (IRE), Canada (AECL/Nordion), the Netherlands (Covidien) and South Africa (NTP). After irradiation in the reactor, the target is digested in acid or alkaline solutions and 99Mo is recovered through a series of extraction (separation) and purification steps and then is shipped to radio-pharmacies, hospitals and clinics. [15]

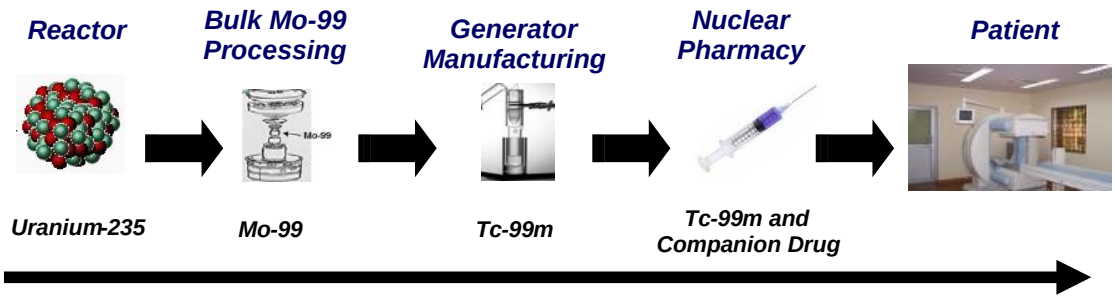

Figure 11. Tc-99m Supply Chain (Natural Resources Canada, 2009a)

7.1.7 Daily extraction of [^{99m}Tc] TcO4− from generators has come to define community expectations of availability and workflow when dealing with ^{99m}Tc- based radiopharmaceuticals. Mo-99 must be produced frequently, which adds to the complexity of ensuring security of supply. An interruption in the production of Tc-99m may take up to one week before the impact is felt by hospitals. Once production is restarted, it may take up to another week before Tc-99m reaches hospitals since it takes a minimum of six days to irradiate targets, process Mo-99 and produce a generator.[16]

7.1.8 By leveraging the existing infrastructure of legacy research reactors, the fission of enriched ^{235}U has long been a cost- effective approach to produce large quantities of high- specific- activity ^{99}Mo. Due to this widespread availability of 99mTechnetium (^{99m}Tc) generators supplied from fission production of 99-Molybdenum (^{99}Mo), alternative sources of supply such as the production of technetium radioisotopes directly from conventional medical cyclotrons has long been neglected.[17,18,19]

7.1.9 Demographic and medical trends suggest that, at least in the near future, global demand for ^{99m}Tc will grow at an average annual rate of 3–8% as these diagnostic imaging procedures expand to new markets, such as those in Asia. However, the research reactors used to irradiate targets that produce most of the world's supply of ^{99}Mo are over 40 years old. The fragility of 99Mo supply has recently come to light during recent shutdowns at two leading production sites. These shutdowns were at times exacerbated by concurrent shutdowns of both the National Research Universal (Chalk River, Canada) and the High Flux Reactor (Petten, The Netherlands).Furthermore, the Canadian NRU reactor, which supplies 35%–40% of the global demand of ^{99}Mo, will terminate its isotope production service in 2016. Other reactors supplying ^{99}Mo are typically more than 40 years old and are at risk of prolonged or permanent shutdown in the near future, creating a risk for loss of a long-term, stable supply of ^{99}Mo for medical purposes.

7.1.10 These interruptions prompted international organizations and several government agencies to step up efforts to find both short and long term solutions to supply shortages and find alternative sources of ^{99m}Tc.[20] However, the cost of building new nuclear reactors for isotope production is extremely high and when coupled to a requirement of full cost recovery on radioisotope production future prices of reactor- sourced ^{99}Mo are estimated to rise dramatically. This price increase will be compounded by the effects of a shift from highly enriched uranium (HEU) to low enriched uranium (LEU) targets for 99Mo production. Moreover, another main disadvantage except of the high cost is the generation of large quantities of highly radioactive waste.

7.1.11 Much research work is thus in progress on the study of alternative methods for the production of ^{99m}Tc in quantities and with the degree of purity required for clinical use. Several techniques have been indicated as extremely promising; such as , the utilization of charged particle accelerators, be they LINAC's or cyclotrons, has been discussed as a potential alternative technology to the fission route. However these methods require specialized instrumentation and complex operations to be performed handling activated materials in order to recover irradiated Mo. Although several groups (Morley, et al., 2012; Gagnon, et al., 2011; Hanemaayer, et al., 2014; Richards, et al., 2013; Qaim, et al., 2014; Lebeda, et al., 2012; Lucconi, et al., 2013) have already investigated alternative techniques, a reliable production methodology is far from being established and this aspect is still an open issue.[25] These discussions have been prompted by basic research concerns as well as the need to explore new production routes to offset the perceived situation of future problems with the availability of 99Mo if no new dedicated reactors are licensed.

7.1.12 Direct production of 99mTc via the ^{100}Mo(p,2n)^{99m}Tc reaction can be considered as one of such alternatives and several works have already proved its feasibility using medical cyclotrons accelerating protons in the range 16-24MeV. By taking advantage of this alterative, as medical cyclotrons are well established worldwide for the production of PET isotopes we do not need to reinvent 50 years of radiopharmaceutical development. Moreover ,one the main advantage of the direct production of 99mTc using cyclotrons, is its low environmental hazards and less waste management difficulties relative to fission-product method, but, on the other hand, the direct production method can only be used for local applications (due to the relatively short half-life of 99mTc -6.02 h), and so a robust and reliable production process leading to a target capable of withstanding high beam currents ,long irradiation time and granting the production of large amounts of 99mTc ,would be necessary.

7.1.13 The feasibility of ^{99m}Tc production with a cyclotron was first demonstrated in 1971 by Beaver and Hupf [21] and confirmed by a number of researchers. In 1971, Beaver and Hupf first reported the direct production of 99mTc from both natural and enriched 100Mo powder and foil targets. Yields were determined using low level irradiations on stacked Mo foils (13 disks, 0.003 in thick, 79 mg/cm2) with 22 MeV protons over 0.0061 μA.hr and substantiated with 97.42% enriched Al-encapsulated 100Mo powder irradiations at 15.2, 20.2 and 21.4 MeV over 4.6x10- 4 to 2.96x10- 2 μA.hr. Extrapolating these results, the authors suggest a 400 μA, 25 MeV irradiation should produce 14 Ci/hr of 99mTc and 750 mCi/hr of 99Mo. However, given the availability of 99Mo, there was little motivation to explore this production option further, and much of the work done over the past 4 decades has been limited to several groups revisiting and refining the cross sectional probability of the 100Mo (p,x) transformation, followed eventually by the development of practical and large- scale cyclotron production methods upon initiation by the Canadian federal government.

7.1.14 There are currently over 950 small medical cyclotrons manufactured by several companies (ACSI, GE, IBA, Siemens, Sumitomo, Best, etc.) installed around the world. Approximately 550 of these machines operate above 16 MeV and are capable of producing appreciable quantities of ^{99m}Tc. The distribution of these cyclotrons by manufacturers is shown in Figure 12.

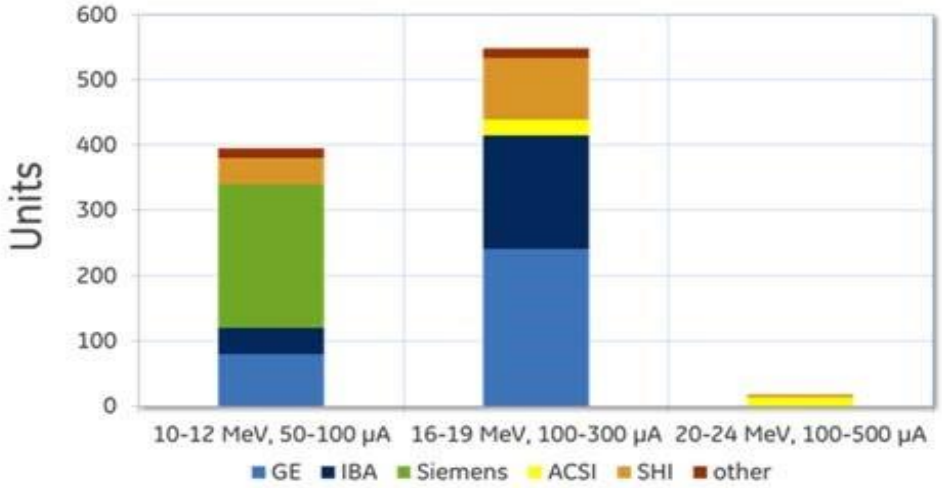

Figure 12. Estimated PET cyclotron numbers by manufacturers

7.1.15 The cyclotron option is based on bombarding Mo-100 targets with protons. The concept is to devise an extraction technique that would allow the Tc-99m to be extracted directly from the irradiated product. This would eliminate the need for Mo-99 generators, but would require a much more efficient and decentralized system to overcome the significantly shorter half-life of Tc-99m, which is six hours compared with the 66-hour half.

7.1.16 The cyclotron option could be viable for a number of reasons. First, it is easily testable with minimal expenditure since the proposed cyclotron facilities are already built and available for testing and eventually for production. Second, with successful process demonstration and target development, this option is scalable and the cyclotrons may be used as multi-use facilities since they are primarily qualified for producing PET and other isotopes. Finally, communication and collaboration between medical cyclotron operators could ensure redundancy in supply and avoid single point of failure in the supply chain. Although each cyclotron serves a limited geographical area, the failure of one would have only a limited impact on the overall market.[22]

8. Chapter 4 Design of a simple low power target for irradiation of pellets

8.1 Scope - Design of a simple low power target for irradiation of pellets

8.1.1 The purpose of this project was to develop a new design of target disc for the direct production of ^{99m}Tc from the cyclotron beam of energetic protons using ^{100}Mo (p, 2n) ^{99m}Tc nuclear reaction.

8.1.2 Hence, the primary scope of this study was to design and develop a low-cost target disc, which could be produced through a relatively fast and easy methodology in a local laboratory.

8.1.3 It should be noted that prior to this work, design of these targets was purely empirical, which required a significant amount of trial and error, long lead times and no guarantee of an optimal design. Thus, a detailed model of the solid target disc, including a target backing and an upper part, was created.

8.1.4 The widely known and diffused package Solidworks Solidworks was used to design an optimized target for the cyclotron at the S. Orsola-Malpighi University Hospital (Bologna, IT). In particular, Solidworks was chosen because it is ideal to create a full solid model in a simulated environment for both design and analysis.

8.1.5 The material requirements are as follows:

- The target backing material should be a high in strength with high heat conductivity which can be cooled by water in order to accommodate the highest heat input without exceeding thermal limit.
- The thickness of the plate support should be kept as thin as is practically possible to facilitate the heat dissipation, but thick enough to guarantee sufficient mechanical strength to withstand the pressure of the cooling water and the structural rigidity to compress the sealing materials.

8.1.6 Furthermore, a number of physical and chemical properties were taken into account in order to reach the best design solution.

- The parts of the assembly which hold the target material must be as non-reactive as possible to the gamma and neutron fields created during the bombardment.
- They should have excellent machining properties, be capable of attaining a good surface finish, and have sufficient mechanical properties for the structural requirements.
- They must also have good cooling properties. They must have thermal properties that prevent them from deforming or melting during bombardment,
- They should be inert to all chemicals they may be in contact with during normal operation.

8.1.7 The new target system is made of two parts:

- A support (or backing), aimed to contain the effective target material (a synthesized pellet, or metal foil, etc.), and is cooled in the back side by a water circuit;
- A front piece that allows to keep the target material in position and should be able to avoid leakage of the Helium that is cooling the front side of the disc

8.1.8 Firstly, a copper alloy target disc was designed by Solidworks 3D solid modelling package. The final design was constructed upon that design.

8.1.9 Copper alloy was selected as the initial testing material, because is relatively inexpensive and easy to be constructed. In future work, after real testing with the beam on copper prototypes it can be changed to a less reactive material like Niobium. The target disc is designed exactly as a low power target so to keep the target material in position by a mechanical action, without any mean lice plating or spluttering that fixes the material on the backing. The dissipated beam power can be removed by enforced cooling from the back-side of the target. To keep the power density low the beam strikes the target under an angle of 5˚–7˚. Thus the temperature on the target surface is kept low. Therefore, a typical material for these requirements is copper alloy.

8.2 Operation

8.2.1 The target assembly is bombarded with energetic protons and the nuclear reaction occurs. The reaction converts only a small percentage of the enriched target material into the product isotope, leaving the remaining target material available to be reclaimed (recycled). The radioactive target disk is typically placed in an appropriate solution (e.g. an acid or oxygen peroxide). The solution is then processed and neutralized and the product is attached (labelled) to a biological molecule of interest.

8.3 Alternate Designs

8.3.1 In the process of researching the best design solution, several design approaches were considered. These are as follows:

A. First option - Initial design concept

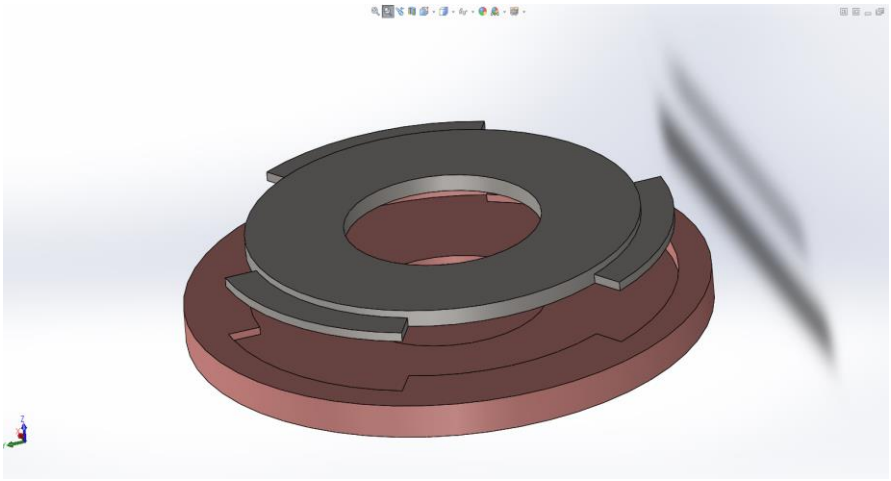

Figure 13. The target disc ,the target backing and the upper part

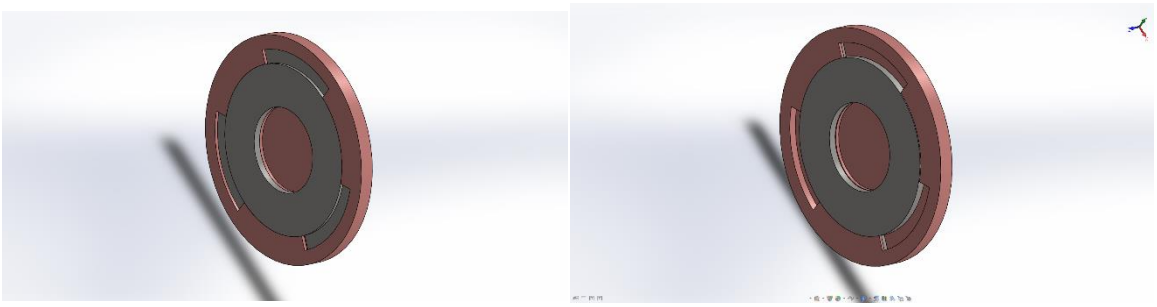

Figure 14 . View of the mounting and locking of two parts

8.3.2 The target backing (with a diameter of 32mm and width of 2mm) consists of a central base (diameter 13mm, depth 0.2mm) in which the irradiated material is being inserted. The target backing has an opening on its upper part (in particular 3 cavities) in which the three blades of the smaller thin window (with a diameter of 24 mm) fit as the second is inserted and being rotated.

8.3.3 The benefit of this design is the optimal fitting of the two parts of the assembly which would constitute an advantage during bombardment.

8.3.4 However, this design has the serious limitation of not allowing an easy removal of the target material. This would potentially expose operators to excessive radiation as they worked to disassemble the irradiated target disk. Also, the difficulty of realistic construction of the front piece because of its very thin blades (width of 0,55 mm, area 27,23 mm2) with a resulting failure to mechanical stresses due to repeated mounting and dismounting led to non-realization of this concept.

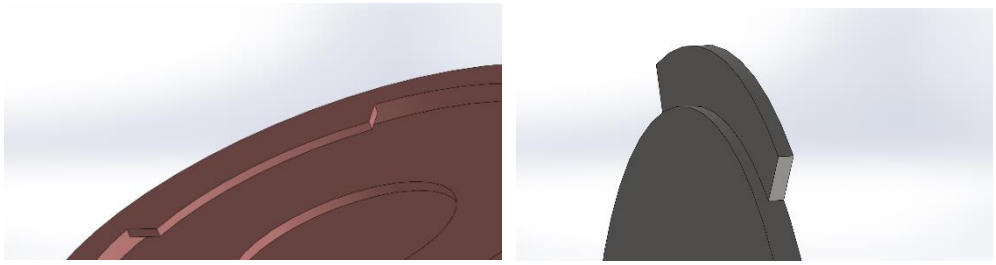

Figure 15 . View of the cavities in which the blades (next) are being inserted

B. Second option

8.3.5 The second design option is shown in fig 4.4 below:

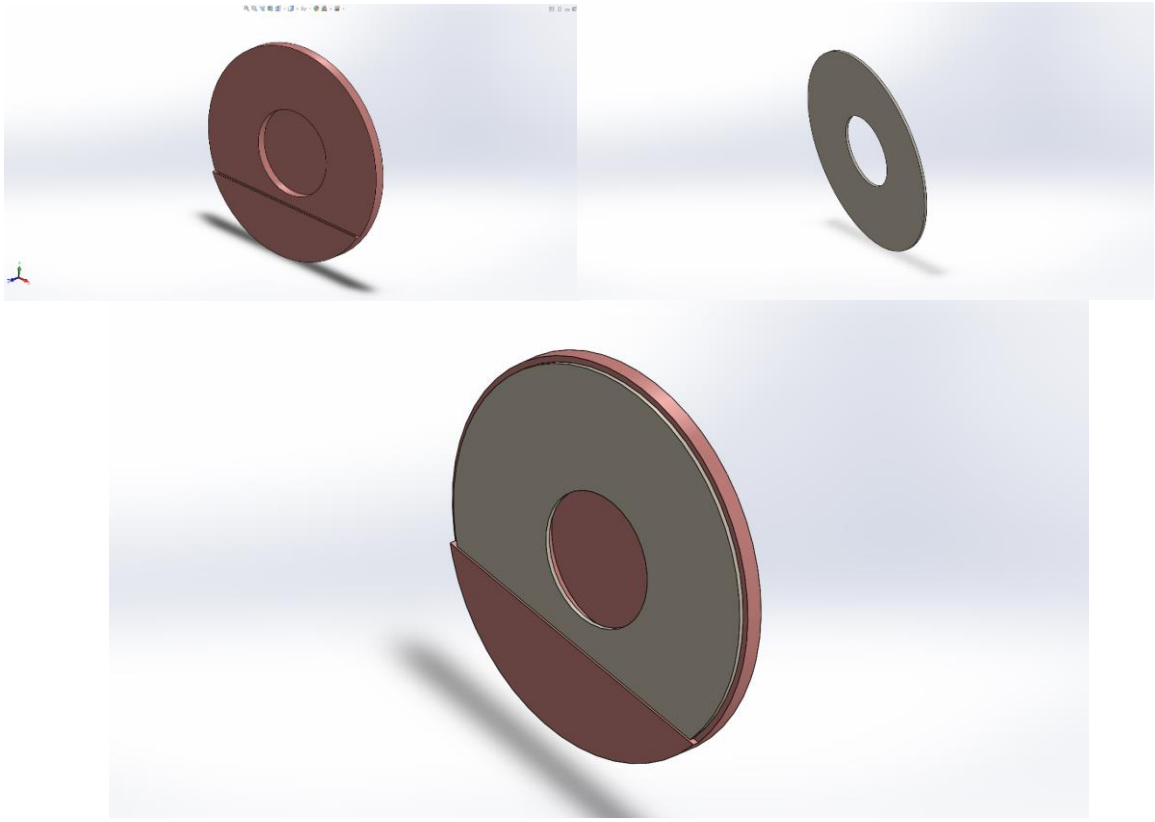

Figure 16. The target disc ,the target backing and the upper part

8.3.6 The target backing (with a diameter of 32mm and width of 2mm) has a pocket on its surface in which a simple thin window (diameter 31mm, width 0,4mm) is being inserted.

8.3.7 The main disadvantage of this concept is the non-ideal fitting of the two parts of the target assembly (a very small area of the window is inserted in the target backing) a fact that could lead in serious problems during the bombardment.

8.4 Description of the final design

8.4.1 Finally, the inception of the successful design was based on the optimization of the first concept. As a matter of fact, the external blades were replaced by two extrusions in the internal surface of the upper part of the target assembly with the appropriate dimensions to be effectively machined. As can be clearly observed, the target base consists of ,not only the corresponding hollows but also an extrusion (0.5mm width,1mm height) in the peripheral resulting in an optimal fitting between the two parts of the assembly.

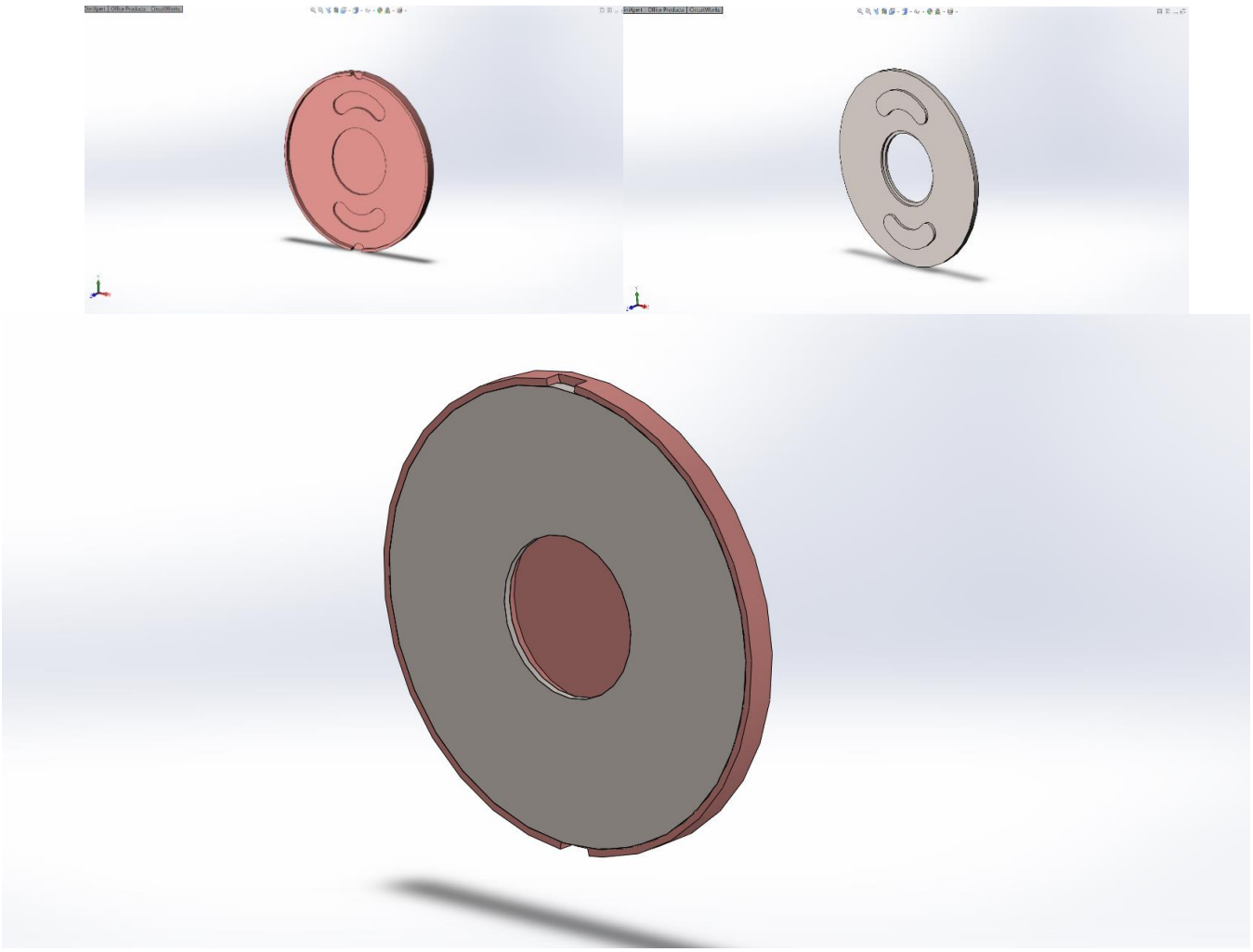

Figure 17. The target disc ,the target backing and the upper part

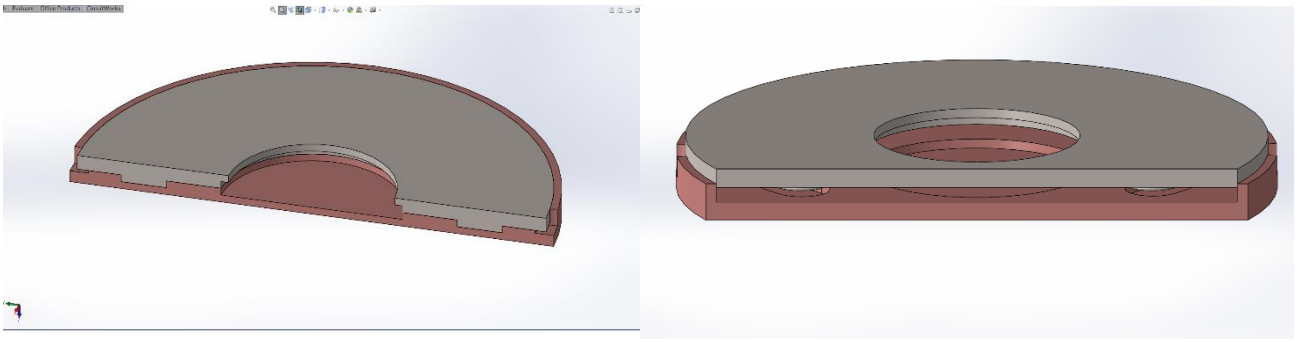

Figure 18. sections presenting the mounting of the assembly

8.4.2 In order to achieve a successful dismounting of the two parts after the irradiation two slots were designed. With the use of a pincer the thin window metal will be easily removed. The design that accomplished all of the key design requirements is illustrated in the next figures.

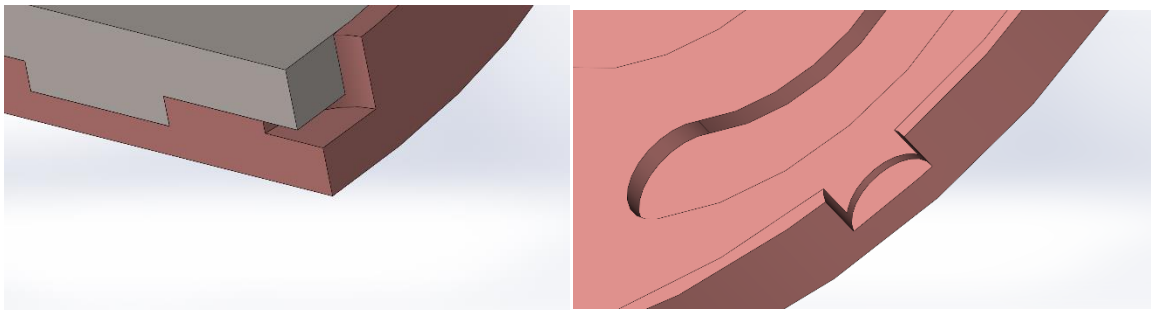

Figure 19. The slots for an effective dismounting of the two parts

8.4.3 Figures 4.8 and 4.9 below present the detailed drawings which were sent to the mechanical laboratory for the speciments to be constructed accordingly.

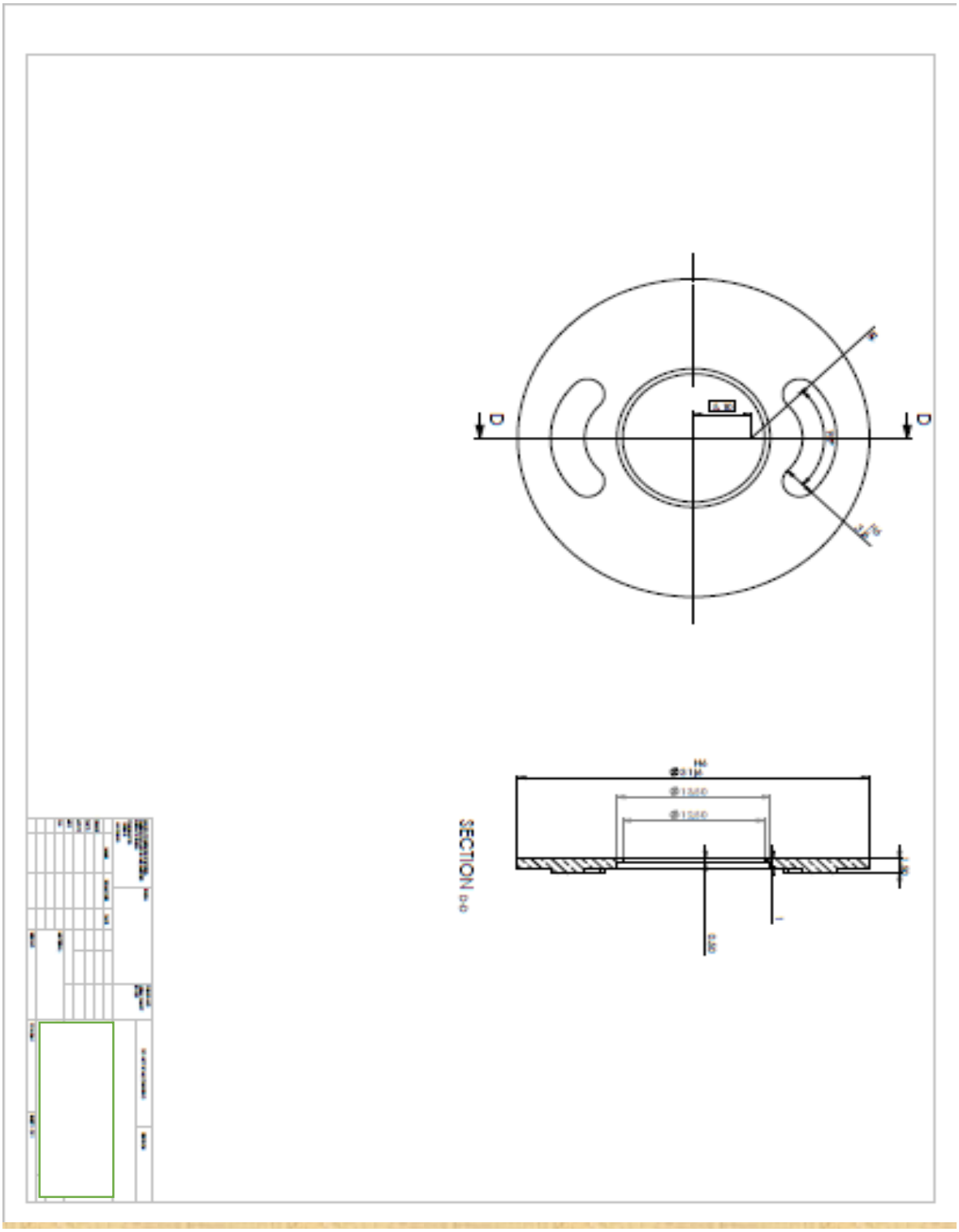

Figure 20. Drawing of the upper part

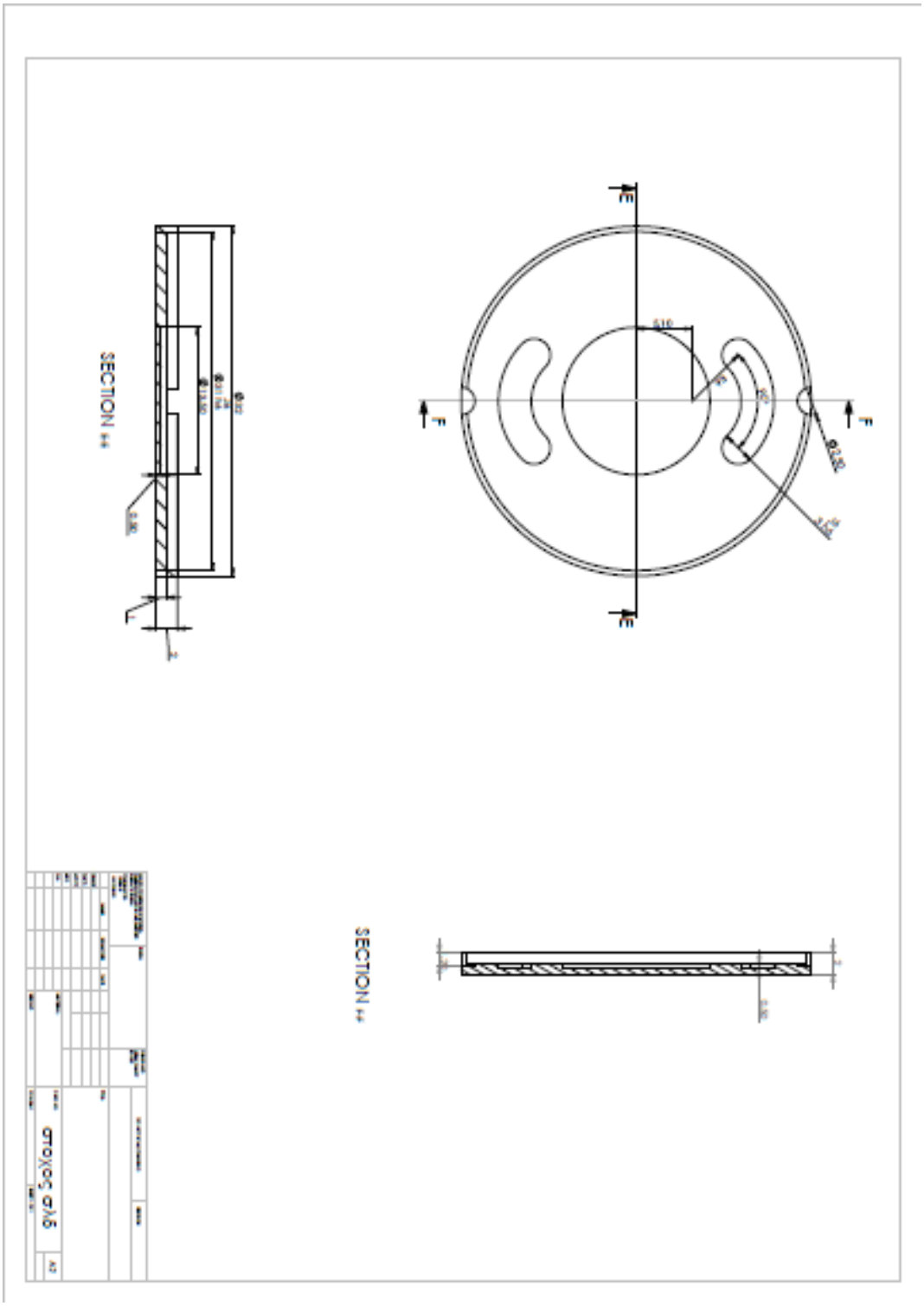

Figure 21. Drawing of the target backing

8.4.4 The figure 22 below present the target disc and each part separately as were constructed.

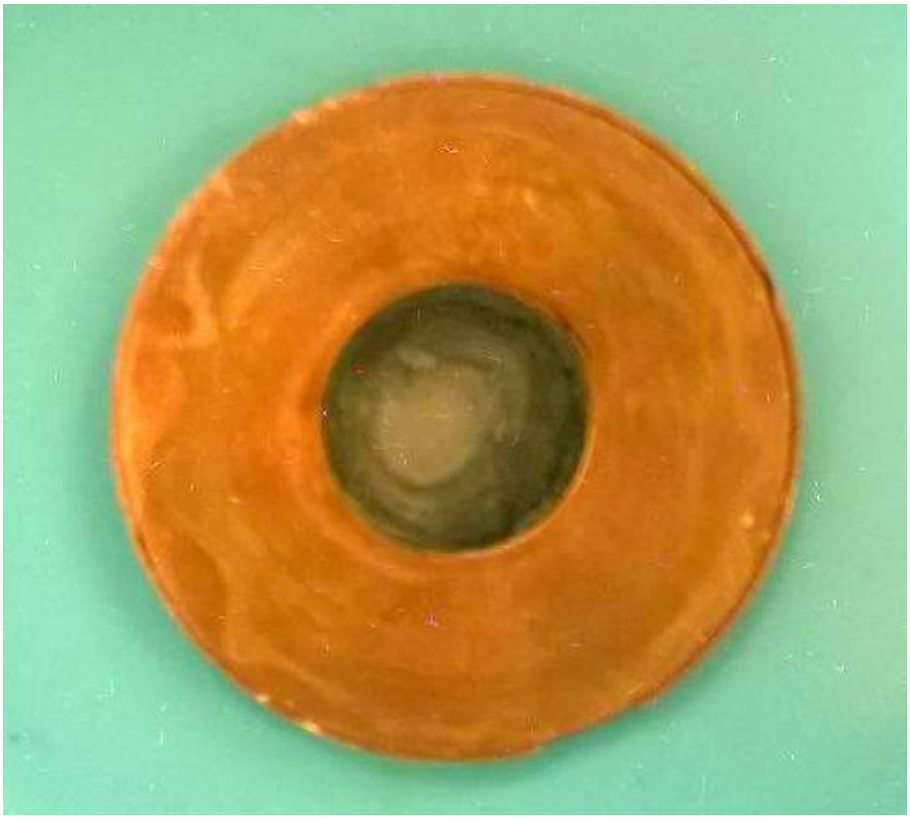

Figure 22. The target backing and the upper part as were cnstructed

8.4.5 For the design verification and validation, a testing plan was created which incorporated specification of the applicable operational parameters as well as the acceptable performance criteria. These are:

- Stress analysis
- Thermal analysis.

8.5 Stress analysis

8.5.1 By reviewing the usage of a very similar existing technological solution, it has been concluded that practically no structural stress is applied to any of the parts of the apparatus, either during the initial fitting, or during the radiation bombardment. Tolerances for the manufacturing of the parts have been selected so as to result in a clearance fit. This, along with the fact that both parts are of the same material and therefore have the same coefficient of thermal expansion, ensures that there will be also no structural stress applied on the parts during the disassembly after the radiation bombardment, when the parts have undergone said thermal expansion. The need for a specific to this apparatus structural stress test is therefore voided and it can also be safely predicted that it will perform as expected in usual working conditions.

8.5.2 The thermal analysis of the new design is presented to the next chapter.

9. Chapter 5 Thermal simulation of the target

9.1 Overview

9.1.1 This chapter presents the thermal analysis of our model. Thermal analysis calculates the temperature and heat transfer within and between the two components of the target assembly and its environment while the irradiation occurs and also the heat removal after the irradiation. This is an important consideration for product safety; if a component gets too hot, a reconsideration of its design or material should be necessary.

9.2 Background information

9.2.1 The heat deposition is linear with beam current, thus the amount of heat that can be effectively handled by the target design directly affects the production capacity of the target. A common method of dealing with poor thermal design is to limit the beam current to very low levels. Thus, for future work, in order to meet the required production rates, it is necessary to optimize this design to withstand the maximum beam current that can be produced on the cyclotron.

9.2.2 Heat transfer processes are classified into three types. The first is conduction, which is defined as transfer of heat occurring through intervening matter without bulk motion of the matter. The second heat transfer process is convection, or heat transfer due to a flowing fluid (a gas or a liquid) .The third process is radiation or transmission of energy through space without the necessary presence of matter. Our study is based on convection heat transfer between the helium, water fluids and the material of target assembly.

9.3 Thermal analysis parameters

9.3.1 In this chapter, the heat flow through the components by a beam of protons with a low energy of 16.5 MeV and a current beam of 30 μA was studied.

9.3.2 There were many aspects that were carefully analysed and understood, these were:

- Temperature of the target chamber
- Time of irradiation
- Power heat
- Thermal distribution
- Heat flow.

9.4 Convective heat transfer

9.4.1 According to thermodynamics, heat energy transferred between a surface and a moving fluid at different temperatures is known as convection. Convection states that the rate of heat loss of a body is proportional to the difference in temperatures between the body and its surroundings.

9.4.2 In reality this is a combination of diffusion and bulk motion of molecules.

- Near the surface the fluid velocity is low, and diffusion dominates.
- Away from the surface, bulk motion increases the influence and dominates.

9.4.3 The convective heat transfer coefficient depends upon physical properties of the fluid such as temperature and the physical situation in which convection occurs.

9.4.4 The specification of convection coefficient is a necessity in thermal applications when cooling of surfaces in contact with fluids occurs and so a thermal convection mechanism takes place .Forced convection occurs when a fluid flow is induced by an external force, such as a pump, fan or a mixer. Respectively, in the cyclotron production the compressor for high-speed recirculation of the helium gas and water convectively absorb heat from the target assembly.

9.4.5 Typical convective heat transfer coefficient for some common fluids [5]:

- Free Convection - air, gases and dry vapors : 0.5 - 1000 (W/(m^2K))
- Free Convection - water and liquids: 50 - 3000 (W/(m^2K))
- Forced Convection - air, gases and dry vapors: 10 - 1000 (W/(m^2K))
- Forced Convection - water and liquids: 50 - 10000 (W/(m2K))
- Forced Convection - liquid metals: 5000 - 40000 (W/(m^2K))
- Boiling Water : 3.000 - 100.000 (W/(m^2K))
- Condensing Water Vapor: 5.000 - 100.000 (W/(m^2K))

9.4.6 For the purpose of the simulation we estimated the convection coefficient parameters as follows:

- Water convection coefficient: h=5000 W/(m^2K)
- Helium convection coefficient: h= 500(W/(m^2K))

9.4.7 The above values were based on the following consideration. After careful thought consultation with the lab staff, and considering the relatively mild impact of this parameter on the results of the thermal study these values were selected, which is well within range for this type of procedure and also within the acceptable margin for error.

9.5 Temperature of the target chamber

9.5.1 The Initial temperature value: 22 ºC

9.6 Time of irradiation

9.6.1 The target was irradiated for 30 seconds, a sufficient time for the target assembly to reach thermal equilibrium.

9.7 Power heat

9.7.1 According to in Equation 5.1 below, the heat input (Q) to the target is a function of the beam current and the energy of the incident protons (5.1)

$$\dot{Q}(Watts) = I\ (\mu A) \cdot \left(\frac{10^{-6}\ \frac{C}{s}}{1\ \mu A}\right) \cdot \left(\frac{1}{1{,}6 \cdot 10^{-19}\ C/p^{+}}\right) \cdot E_p(Mev/p^{+}) \cdot E\left(\frac{1{,}6 \cdot 10^{-13}\ J}{1\ MeV}\right)\left(\frac{W}{1\ J/s}\right)$$

$$\dot{Q}(Watts) = I\ (\mu A) \cdot E_P\ (Mev/p^{+}) \quad (5.1)$$

Equation 5.1- Heat input (Q) to the target

where:

Beam current (*I*): is quantified in micro-amps (μA) and

Proton energy (*E*) : is quantified in mega-electron volts (MeV).

9.7.2 The intended operation conditions for our target were 16.5 MeV protons at a beam current of 30 μA. According to Equation 5.1 this corresponds to a proposed heat input of 495 Watts. The following graph shows the heat current beam.

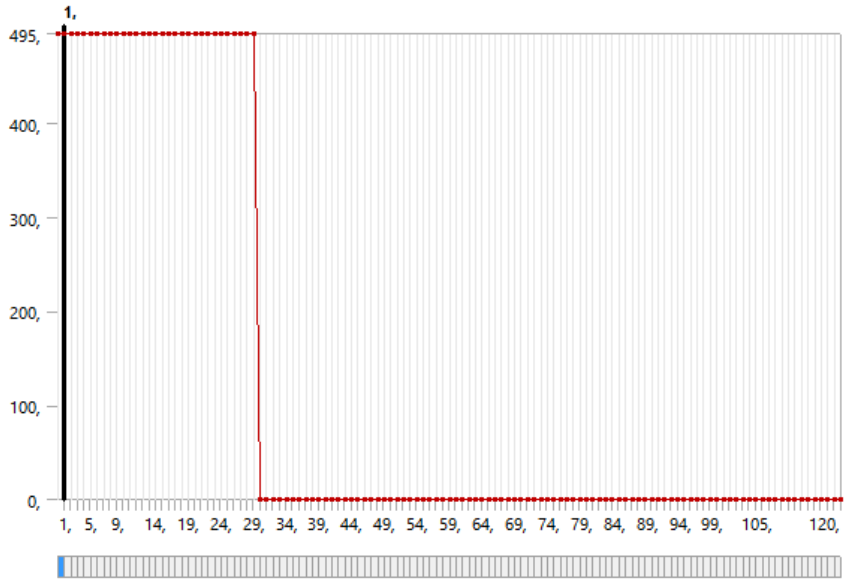

Figure 23. Heat beam of 495 W for 30 sec.

9.8 Experimental description - procedure

9.8.1 As it has been discussed before, the new target system is made of two parts: a support aimed to contain the effective target material and a front piece that allows it to be kept in position and be able to avoid leakage of Helium (which is used for the cooling of the front side of the disc).The target chamber is separated from the vacuum chamber of the cyclotron by two thin havar foils. All target supports (target

material, water to cool the body of the target, helium for the cooling of the metallic foils) enter and leave the target through the rear flange. The optimal cooling configuration maximizes heat removal. This allows for the highest heat input, or highest acceptable beam current and therefore to optimize the production of the desired radionuclide.

9.8.2 The simulations were then performed by considering an irradiation of 30 seconds by a power beam of 495 Watt. The thermal distribution and power heat flux are presented next.

9.8.3 The next figures show the thermal distribution in the target assembly, and separately in the target backing and in the front piece during the irradiation process.

9.9 Results of heat flux and temperature distribution during the 30 seconds of irradiation process

9.9.1 Next figures below show the heat flux during the first 30 seconds that the irradiation occurs. As can be easily observed the majority of the heat is greatest in the center where the power is deposited with a maximum value of heat flux (the rate of heat energy transfer through the surface of the target assembly) 17,082 W/mm^2.

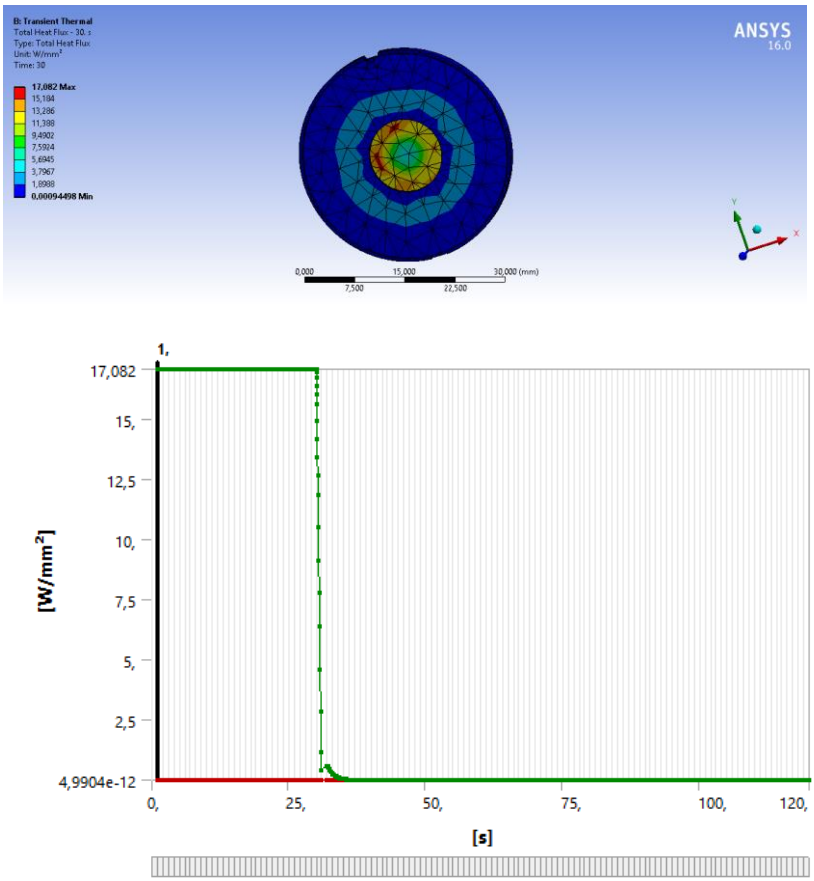

Figure 24. Heat flux during the irradiation

9.9.2 The results obtained (Table 4) show that the temperature on the target assembly ranges from 114,8 ^{o}C to 308,53 ^{o}C ,well below the melting point of the copper alloy material (1084 ^{o}C)

Object Name	Temp-5. s	Temp – 15. s	Temp – 30. s	
Minimum		111,4 °C		
Maximum		308,53 °C		

Table 4. Minimum and maximum temperature during the 30 sec of irradiation

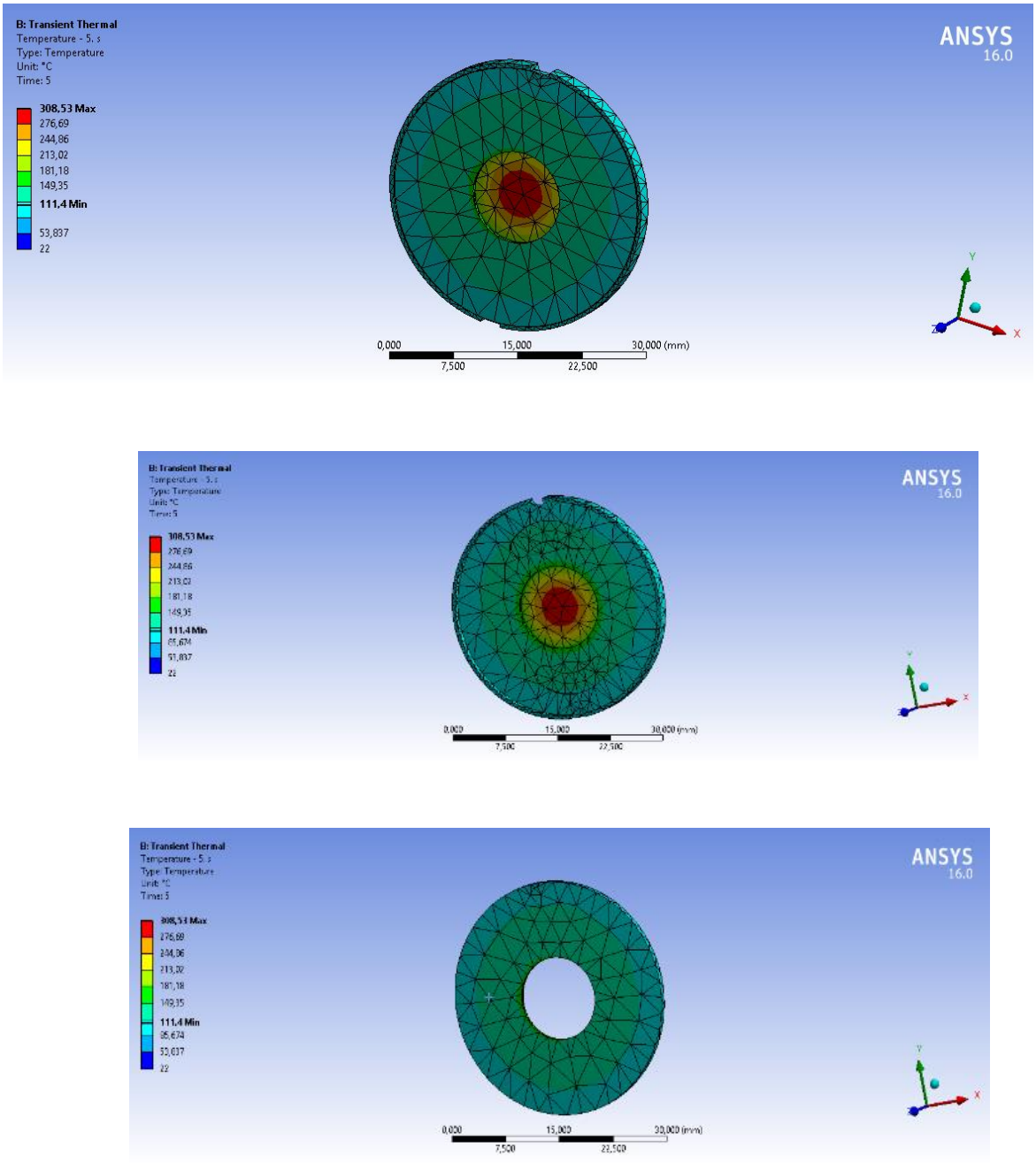

Figure 25. Temperature distribution on the 5th second of irradiation

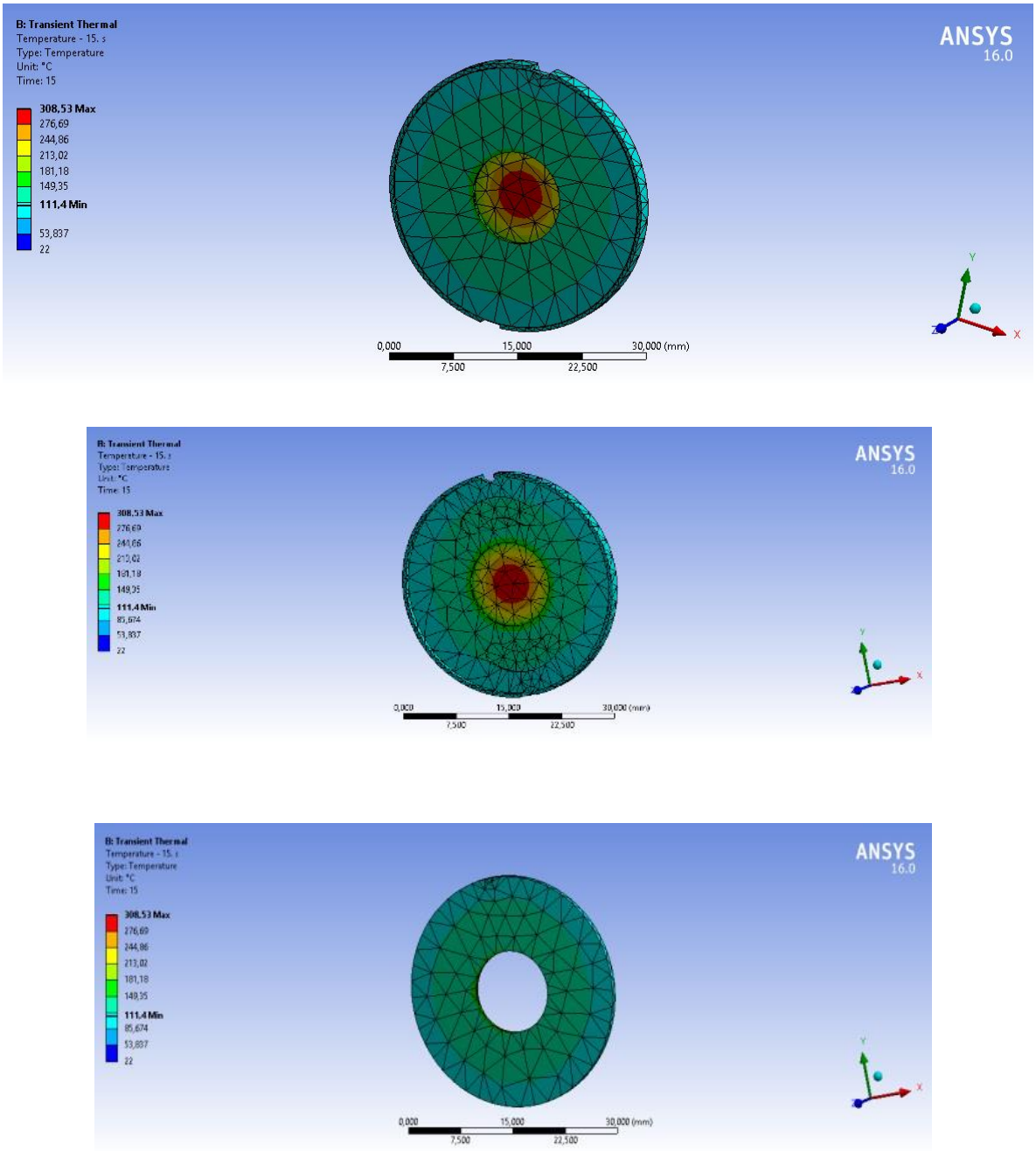

Figure 26. Temperature distribution on the 15th second of irradiation

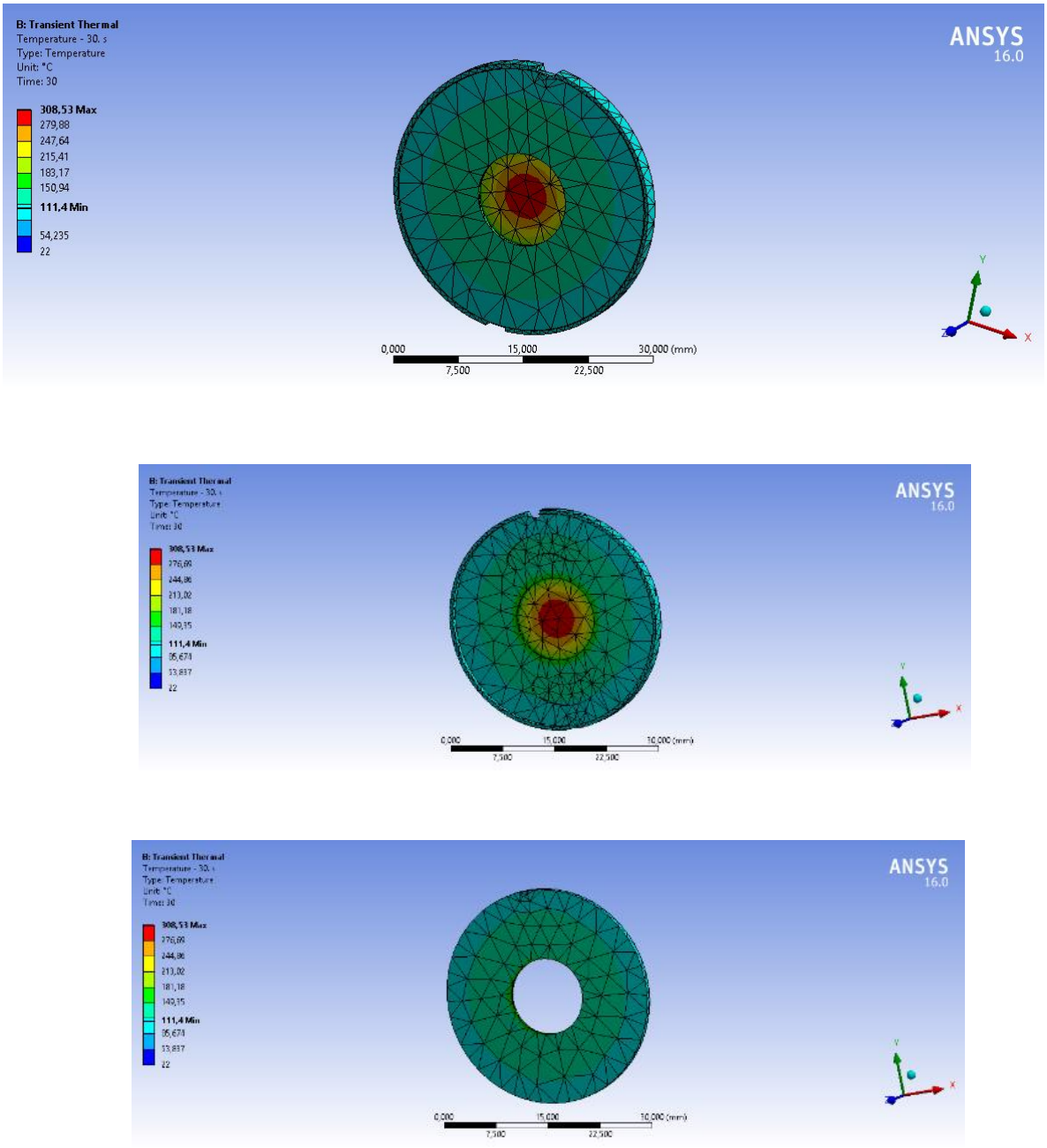

Figure 27. Temperature distribution on the 30th second of irradiation

9.10 Results of heat removal after irradiation process stops (31sec to 35 sec)

9.10.1 The irradiation stops at the 30th second while the helium and water cooling still function in order to succeed the heat removal of the target assembly.

9.10.2 The heat distribution of the next 5 seconds (31sec to 35 sec) is presented below.

Object Name	Temp- 30. s	Temp- 31. s	Temp - 32. s	Temp – 33. s	Temp – 34. s	Temp – 35. s
Minimum	111,4 °C	87,585 °C	51,61 °C	33,97 °C	26,975 °C	24,068 °C
Maximum	308,53 °C	91,273 °C	57,979 °C	37,009 °C	28,239 °C	24,593 °C

Table 5. Temperature decrease during the first 5 seconds after irradiation

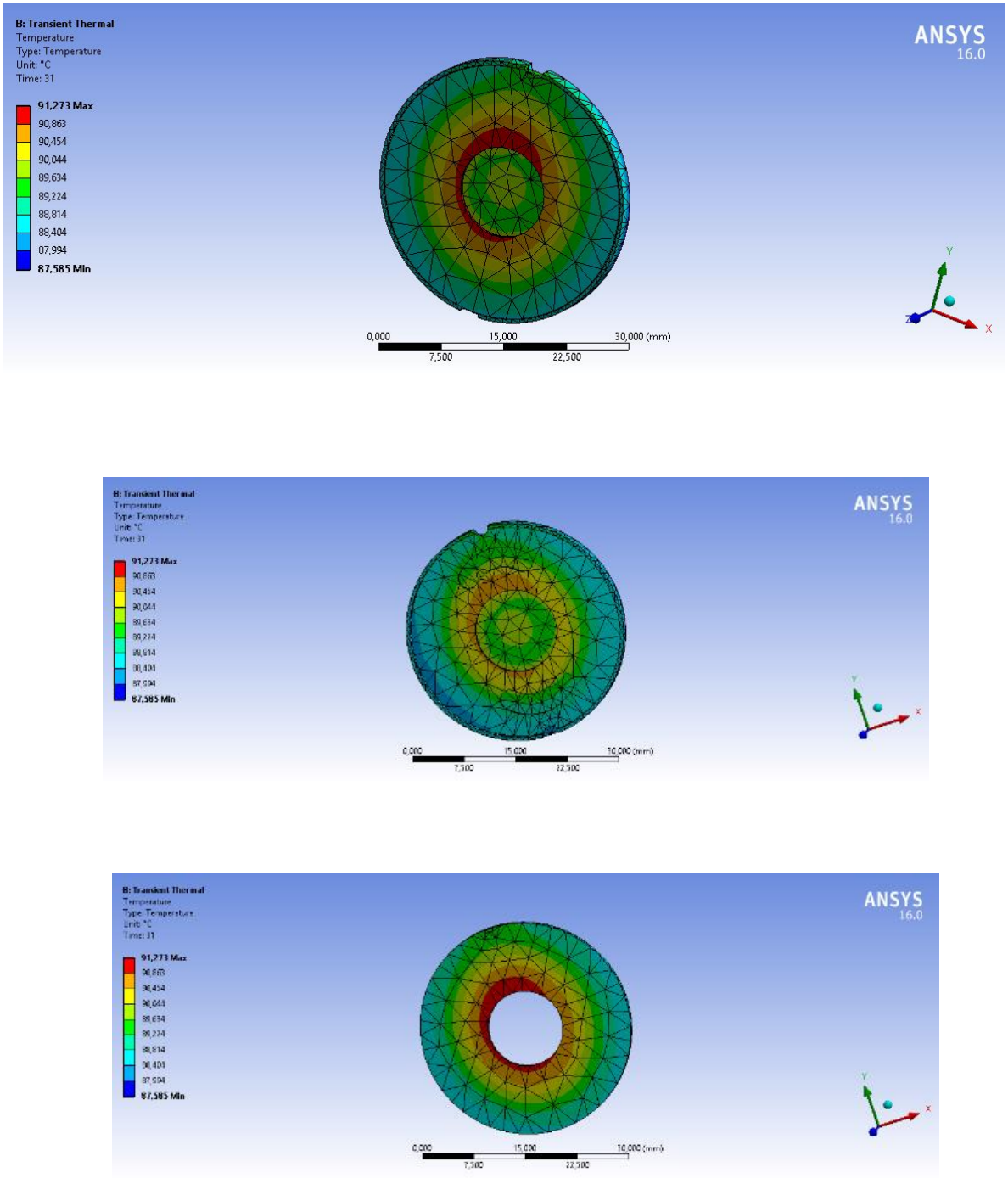

Figure 28 . Temperature distribution on the 1st second after the irradiation (maximum Temperature: 91,273 ^{o}C , minimum Temperature: 87,585 ^{o} C) on the target disc and separately the target backing and the upper part

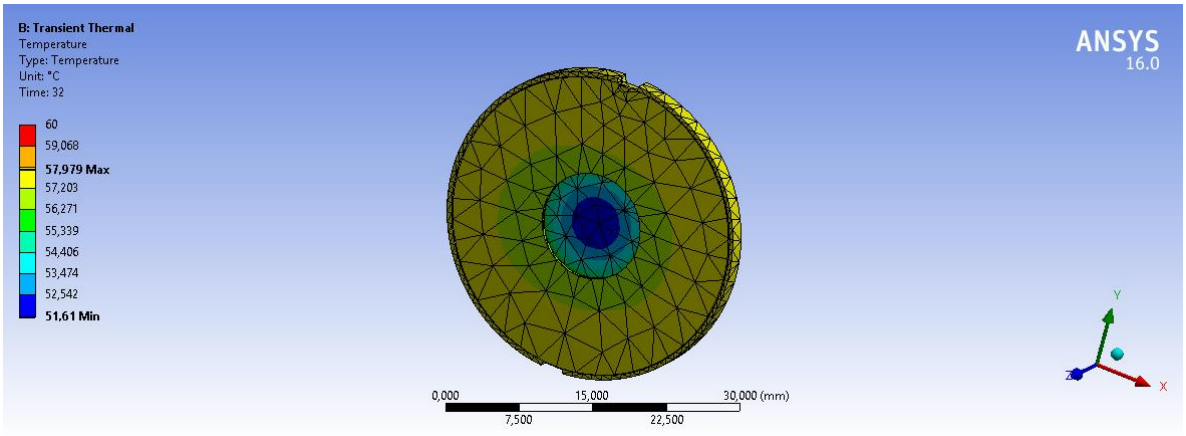

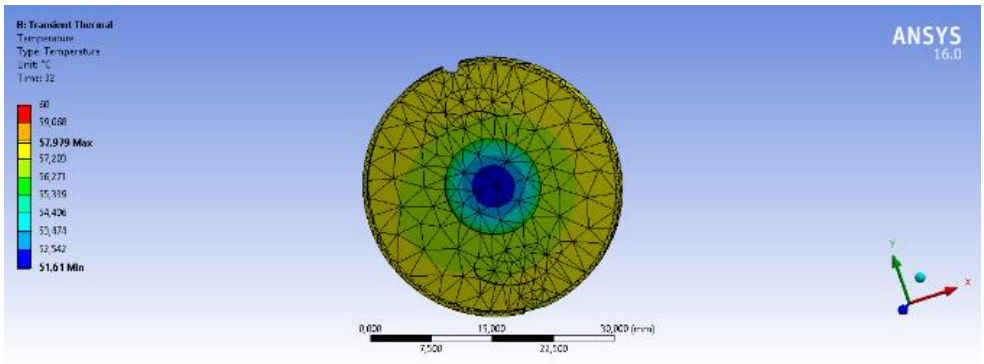

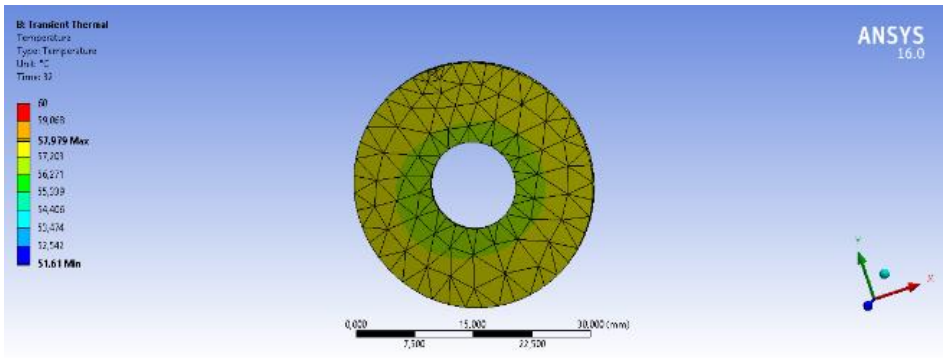

Figure 29 . Temperature distribution on the 2nd second after the irradiation (maximum Temperature: 57,979 ^{o}C , minimum Temperature: 51,61 ^{o} C) on the target disc and separately the target backing and the upper part

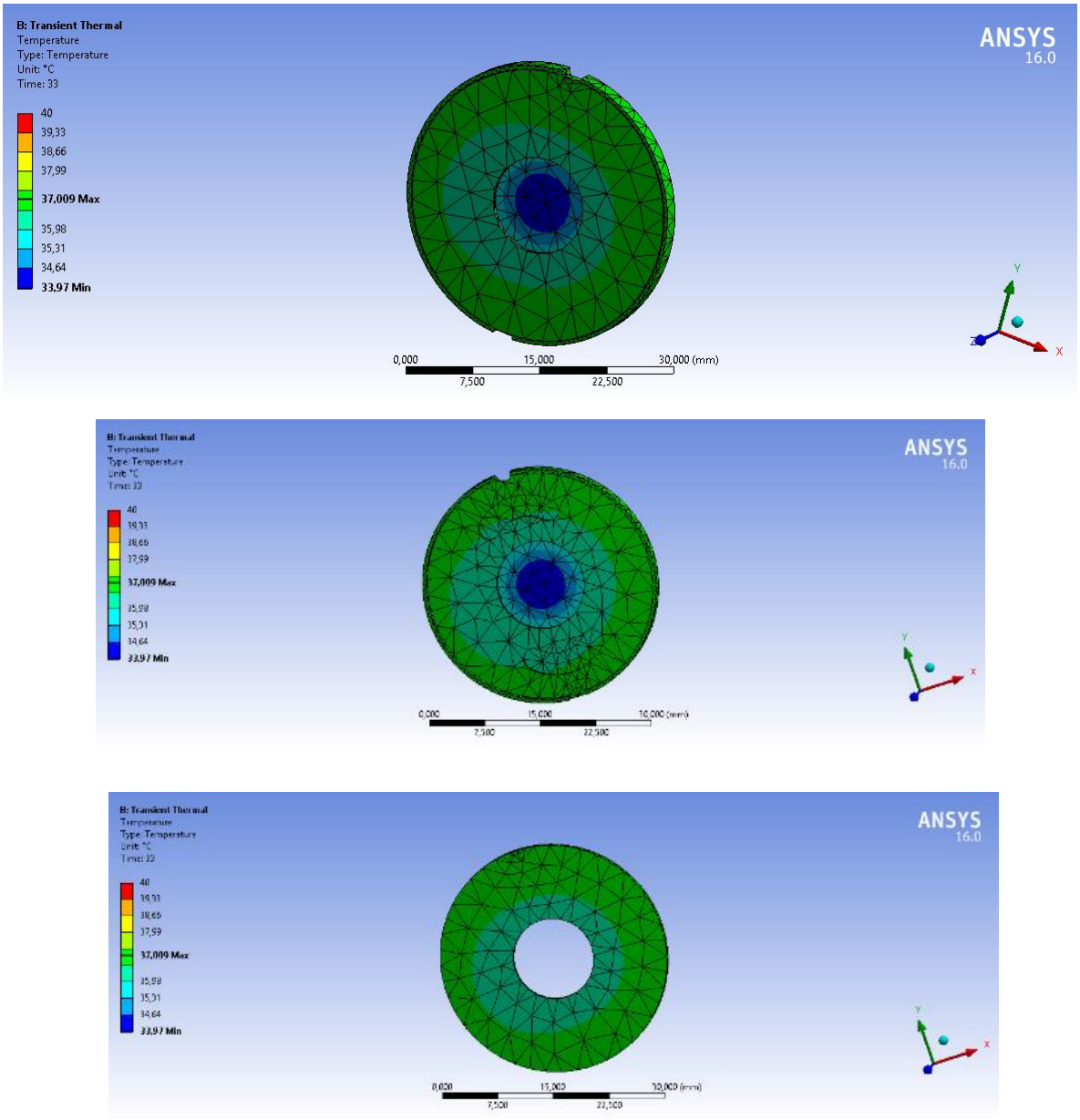

Figure 30 . Temperature distribution on the 3rd second after the irradiation (maximum Tempearature: 37,009 ºC , minimum Temperature: 33,97 º C) on the target disc and separately the target backing and the upper part

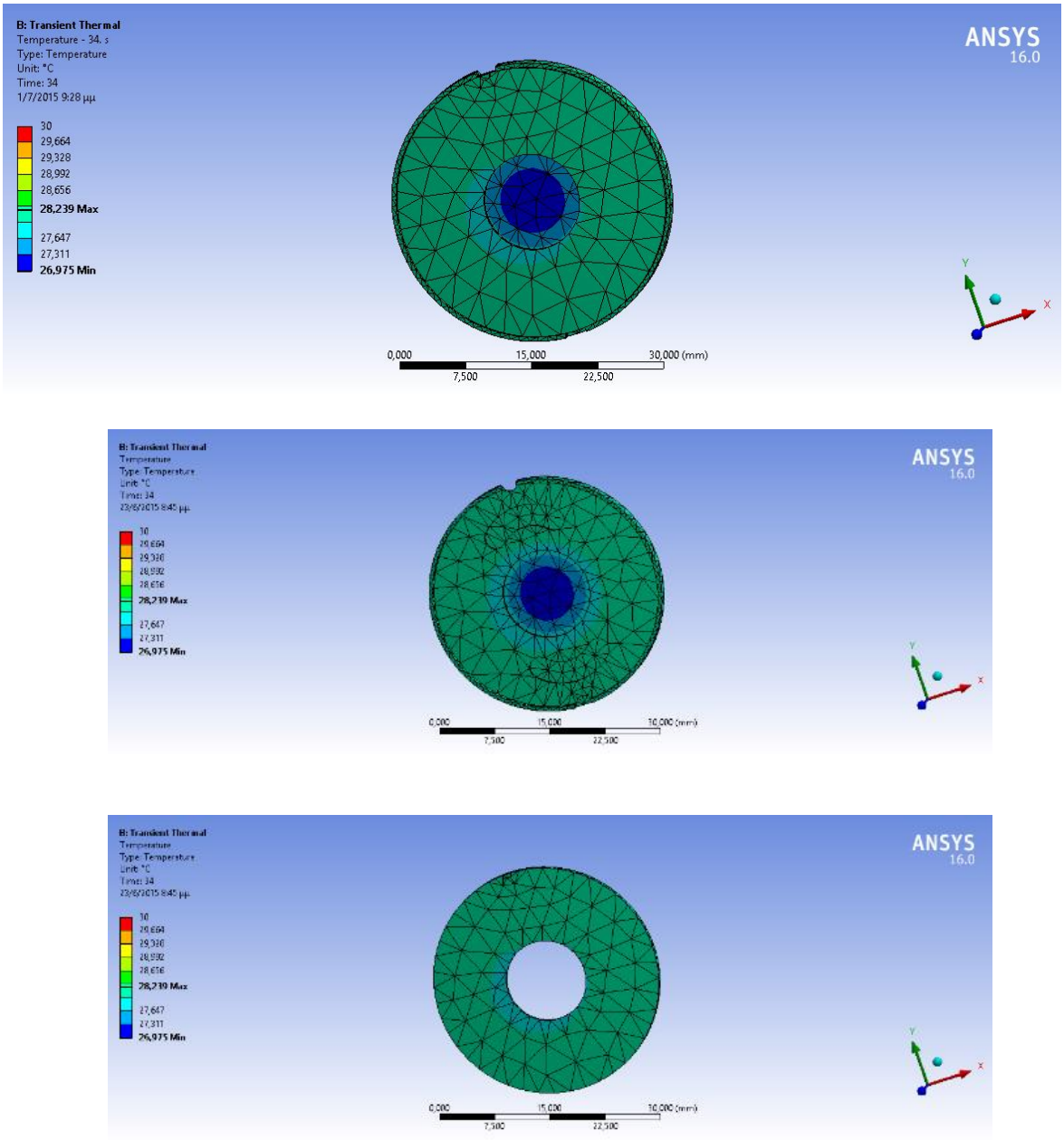

Figure 31 . Temperature distribution on the 4th second after irradiation (maximum Temperature: 28,239 ^{o}C , minimum Tempearture 26,975 ^{o}C) on the target disc and separately the target backing and the upper part

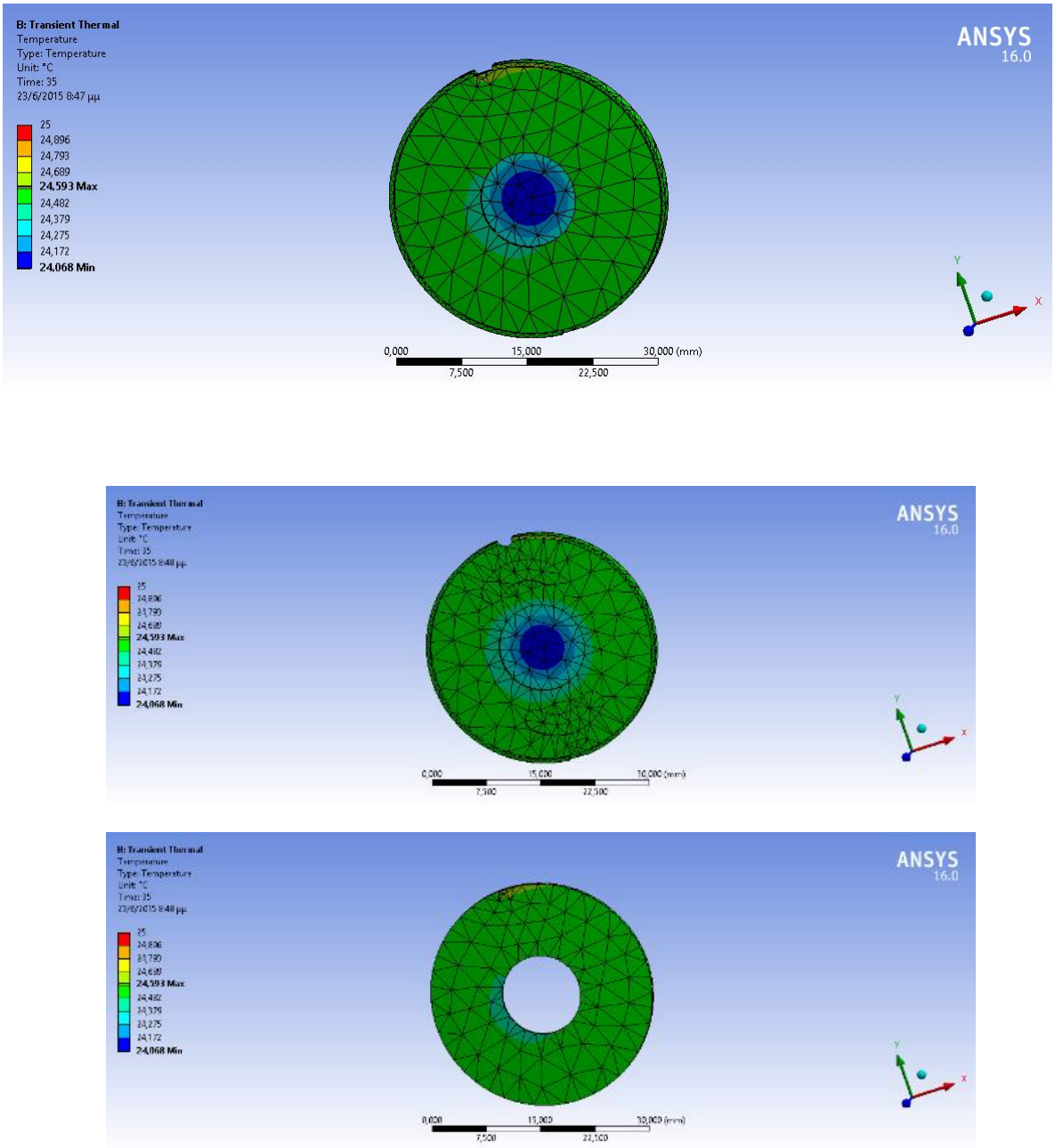

Figure 32 . Temperature distribution on the 5th second after irradiation (maximum Temperature:24,593 ^{o}C , minimum Tempearature: 24,068 ^{o}C) on the target disc and separately the target backing and the upper part

9.10.3 As figures below show the temperature decreases significantly during the first 5 seconds after the irradiation stops and has reached its first value (22^{0}C) at the 44th sec.

9.10.4 It is evident that from the very first second the target assembly loses the 2/3 of its previous temperature (from 308,53 ^{o}C to 91,273 ^{o}C , due to the effective function of helium and water cooling system.

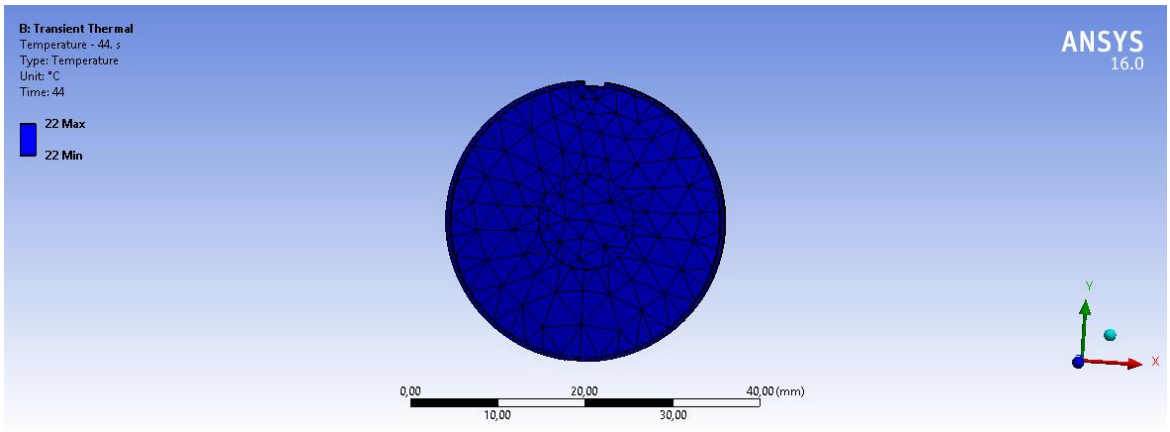

Figure 33 . Temperature on the 44th second reaches its first value 22^{o}C

9.11 Results Discussion

9.11.1 The results showed that during the irradiation process the most of the energy is deposited in the center of the target assembly and maintained constant value (different temperatures through the surface) greater in the target backing where the beam hits and significantly lower as the distance from the center increases. The front piece is affected less as the helium cooling is mostly aimed to avoid any local melting spot, due to local excess of power absorption.

9.11.2 It was evident that the temperatures even near the target face, the most exposed to heat stress, remained well below the material melting temperature (copper melting temperature-1082,3 ^{o}C) which certainly ensures the physical integrity of the target assembly.

9.11.3 Therefore, the results of the thermal analysis indicate that operation of the target system at 30 μA beam current should produce a maximum temperature that has a 'safety factor' of approximately 3 times the melting temperature of copper.

9.11.4 With the results obtained in the performed simulation, it is clear the importance of making a careful analysis of all parameters involved in the irradiation of a solid target, especially with regard to cooling.

10. Chapter 6 Irradiation tests

10.1 Overview – Irradiation tests

10.1.1 The main purpose of this project, as previously discussed is the design and construction of a target support capable to host a variety of materials (pellets, metal foils, etc.) for cyclotron production of ^{99m}Tc in quantities sufficient for local clinical use without requiring complicated and expensive techniques of target preparation.

10.1.2 Therefore, the study was firstly focused to an optimal design of a target backing in which the irradiating material was being inserted and was hold with the upper part.

10.1.3 The planned outcome of this project was the development of ^{99m}Tc production method using the reaction of ^{100}Mo (p,2n)^{99m}Tc in cyclotron .

10.1.4 This chapter describes the initial irradiation test using the prototype designed.

10.2 Preparation procedure

10.2.1 Due to time limitations, only a limited testing of the first prototype of target support was possible.

10.2.2 In this test, the enriched target material used was a series of five ^{100}Mo foils (25 µm thick, area of 1 cm^2) as can been seen in Figure 34. These were stacked into the copper target. The positioning of the foils was successful and the front piece showed to be able to close properly, retaining its original thickness of 2 mm, a fundamental parameter to allow the insertion of the target support into the target chamber.

Figure 34 . 100Mo foils

10.2.3 As it has been discussed before, in order to protect the target material of reaching excessively high temperatures during irradiations, water cooling flow is used across the back of the target assembly while helium cooling flow is used for the front side (Figure 35. In order to avoid any loss from the helium cooling circuit, a thin sheet of Havar material (25 µm thick) was placed between the support and the helium cooling flange.

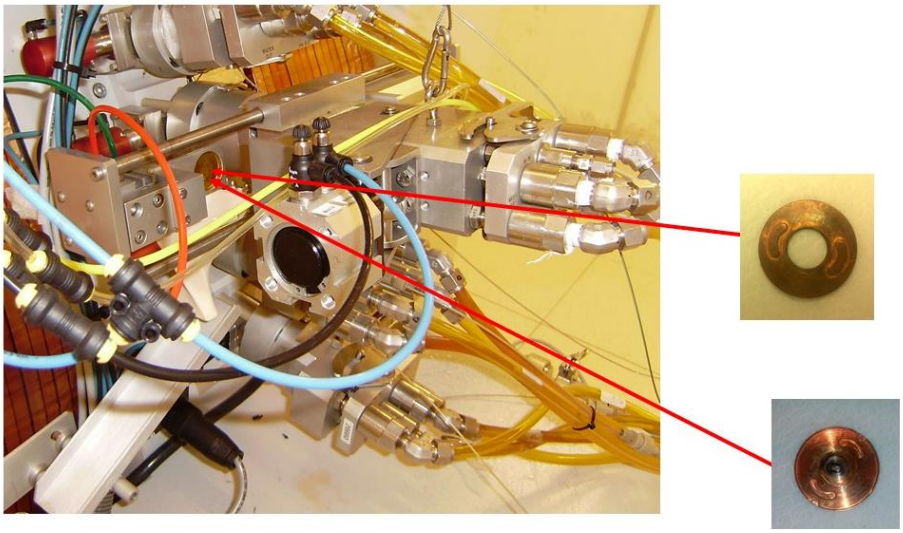

Figure 35. The front piece is cooled by He gas (4 bar), the back piece by deionised water (6t/min)

10.2.4 While the insertion of the target support was successful, an initial test of target tightness (simulating irradiation conditions without accelerating and extracting the beam) showed that the target support was not completely tight and a significant loss of Helium gas had occurred. This could be easily observed, by placing the irradiation line in the same condition of an irradiation; showing that the pressure in the Helium circuit was rapidly decreasing requiring continuous refill from the Helium compressing system.

10.2.5 In these conditions, an irradiation is not safe and cannot be performed. Despite the detail put in the design of the support, the lack of a final sealing (e.g. using an O-ring) proved to be not successful.

10.2.6 Thus, in order to eliminate the leaks and make the test possible, it was decided to improve tightness by adding a thin foil of Havar material (25 μm thick) in front of the support. This would avoid Helium circulation within the body of the support and the helium cooling flange. The repetition of the tightness test with the configuration including the front foil was successful.

10.2.7 Before proceeding to irradiation, a final, long time tightness test was performed for 30 minutes to ensure that no loss of helium gas would occur. The test was successful, and this made possible to proceed with the irradiation process.

10.3 Irradiation experiments

10.3.1 Irradiation was carried out with a current beam of 16.5 MeV proton beam of the cyclotron. Given the additional presence of the thin Havar foil for sealing, the effective energy of the proton beam entering the target was calculated 15.7 MeV.

10.3.2 The target was irradiated for 90 minutes at a current of 20 μA (Ep=15.7 MeV). During the irradiation the temperature of the water cooling circuit was constant at 18.5 ° C.

10.3.3 After irradiation the target assembly was discharged through the automatic transfer system in a safe position, outside the bunker (figure 6.3). The transport was successful and the target support was properly delivered into the shield container.

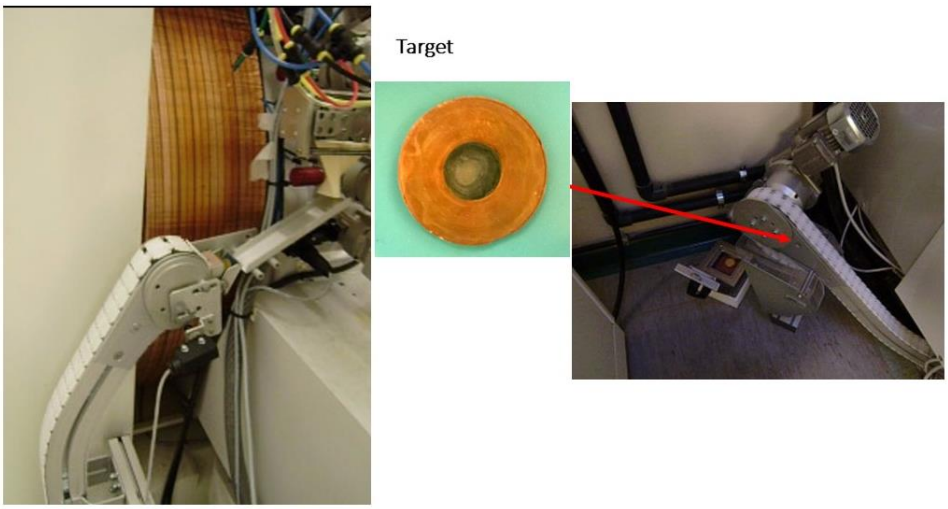

Figure 36 . The automatic expalsion of the target support from the target chamber

10.3.4 The container was then carried to the processing hot cell. In this initial experiment, the target support was disassembled manually; however, this operation can be automated. It is suggested that the automation process could be part of a future improvement.

10.3.5 After disassemble, an activity meter measured the irradiated enriched material's overall produced activity, which resulted to be 3193 Mbq , with an uncertainty of 5 % (due to the calibration of the activity meter).

10.3.6 The sample was then loaded into a previously developed dissolution, separation and purification automated module. The process of dissolution, separation of Technetium from the Molybdenum its starting material and purification was completed in 90 minutes, according specific methods.[23,24]

10.4 Imaging test

10.4.1 A final solution of purified ^{99m}Tc pertechnetate was obtained, with an activity of 686 MBq at 4h.

10.4.2 A sample of 259 MBq was taken from the final solution and injected into a typical phantom for evaluation of the performance in SPECT imaging.

10.4.3 A tomographic acquisition was performed using a Siemens E.cam dual head gamma camera, fitted with Low Energy High resolution collimators. Tomographic acquisition was performed with a matrix 128x12p pixels, 120 angular steps, 30 seconds acquisition per step. Reconstruvision was performed by filtered back projection. An example of selected transaxial images of the SPECT performance phantom is shown in Figure 37.

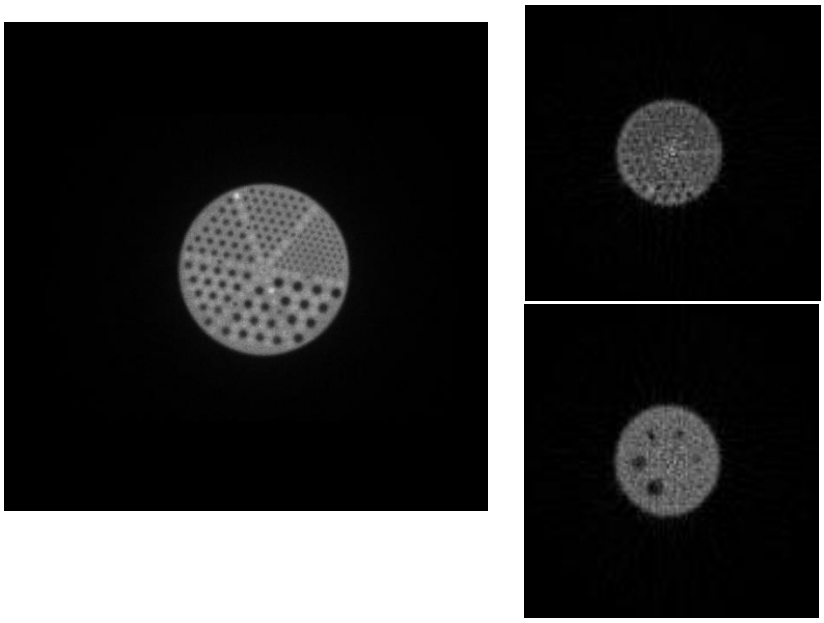

Figure 37. Transaxial images the SPECT performance phantom

10.4.4 It should be noted that the separation and purification technique and quantitative analysis of SPECT imaging was outside the scope of this work.

10.4.5 With regards to the effective contribution of this work to the whole process, it is possible to conclude that it has been proven that the target system developed in this work was proved to be capable to produce clinically relevant activities of 99mTc.

10.4.6 However, future work is still necessary in some areas such as the avoidance of using of sealing foils. This can be done by modifying the design of the target support, in order to host an O-ring or other type of sealing (e.g. Helicolfex); this will require a detailed analysis of the possible materials, and an upgrade of the stress tests here developed.

10.4.7 Furthermore, at this initial stage, Copper was selected as the material of choice, due to its availability, relatively low cost, excellent thermal conductivity and ease of machining. However, it is well known that Copper can significantly be activated in long time with high current irradiations, being hit by the “tails” of the proton beam, or due to interaction of secondary neutrons. Hence, in further developments, other materials could be investigated, such as Titanium, Niobium and others, which have sufficient thermal conductivity, attractive overall mechanical characteristics and limited cross section capable for activation at the energy of biomedical cyclotrons.

10.4.8 In conclusion, this work represented a first step in a new direction of investigation in the design of targetry for cyclotron production of ^{99m}Tc.

11. Conclusions

11.1.1 The primary scope of this study was to design and develop a low-power target disc, which could be produced using relatively fast and easy methodology in a local laboratory.

11.1.2 In this thesis, which was conducted at the Medical Physics Unit of the Bologna Hospital ‘’S. Orsola-Malpighi University Hospital‘’, I designed an optimized target disc for the GE PETrace cyclotron with the use of Solidworks software. In particular, Solidworks was chosen because it’s ideal when creating a full solid model in a simulated environment for both design and analysis.

11.1.3 The development of a low-cost target, producible through a relatively fast and easy methodology and capable of granting a local supply was studied. The new target system is made of two parts: a support (or backing), intended to contain the effective target material and a front piece that keeps the target material in position.

11.1.4 Copper was selected as the material of choice, due to its availability, relatively low cost, excellent thermal conductivity and ease of machining. However, it is well known that Copper can be activated after prolonged exposure to high current irradiations, being hit by the “tails” of the proton beam, or due to interaction of secondary neutrons. Hence, in future work other materials could be investigated, such as Titanium, Niobium and others which have sufficient thermal conductivity, attractive overall mechanical characteristics and limited cross section capable for activation at the energy of biomedical cyclotrons.

11.1.5 For the design verification and validation, a testing plan was created which incorporated specifications of the applicable operational parameters as well as the acceptable performance criteria.

11.1.6 The need for a specific to this apparatus structural stress test is voided in this thesis; by reviewing the usage of a very similar existing technological solution, it has been concluded that practically no structural stress is applied to any of the parts of the apparatus during the initial fitting or during the radiation bombardment. Tolerances for the manufacturing of the parts have been selected so as to result in a clearance fit. This, along with the fact that both parts are of the same material and therefore have the same coefficient of thermal expansion, ensures that there will also be no structural stress applied on the parts during disassembly after radiation bombardment, i.e. when the parts have undergone said thermal expansion.

11.1.7 The heat deposition is linear with beam current, thus the amount of heat that can be effectively handled by the target design directly affects the production capacity of the target. The specification of convection coefficient is a necessity in thermal analysis when cooling of surfaces in contact with fluids occurs and so a thermal convection mechanism takes place. After careful consideration and consultation with the laboratory staff, and taking into account the relatively mild impact of this parameter on the results of the thermal study, the medium values of forced convection coefficient parameter for the water and helium fluid cooling mechanism were selected. Future work would make a more specific calculation regarding these parameters when applied to cooling.

11.1.8 Thermal simulations were performed using Ansys software by considering an irradiation of 30 seconds by a power beam of 495 Watt.

11.1.9 The results showed that the temperatures near the target face - the area most exposed to heat stress - remained well below the material melting temperature

(copper melting temperature -1082,3 ^{o}C) which ensured the physical integrity of the target disc. The front piece is less affected as the helium cooling is mainly intended to avoid any local melting spot due to local excess of power absorption.

11.1.10 The objective of this thesis was the development of ^{99m}Tc production method using the reaction of ^{100}Mo (p,2n)^{99m}Tc in cyclotron.

11.1.11 Due to time limitations, only limited testing of the first prototype of the target support was possible.

11.1.12 The enriched target material used was a series of five ^{100}Mo sheets. Irradiation was carried out with a current beam of 16.5 MeV proton beam of the cyclotron. Given the additional presence of the thin Havar foil for sealing, the effective energy of the proton beam entering the target was calculated as 15.7 MeV.

11.1.13 The target was irradiated for 90 minutes at a current of 20 μA. During the irradiation the temperature of the water cooling circuit was constant at 18.5 °C. A final solution of purified ^{99m}Tc pertechnetate was obtained, with an activity of 686 MBq at 4h.

11.1.14 A sample of 259 MBq was taken from the final solution and injected into a typical phantom for evaluation of the performance in SPECT imaging and a tomographic acquisition was performed using a Siemens E.cam dual head gamma camera, fitted with Low Energy High resolution collimators. Tomographic acquisition was performed with a matrix 128x12p pixels, 120 angular steps and 30 seconds acquisition per step.

11.1.15 In conclusion, this work successfully represented a first step in a new direction of investigation in the design of a low-powered target for cyclotron production of ^{99m}Tc.

References

1. Review of cyclotron used in the production of radioisotopes for biomedical applications, P. W. Schmor
2. The Production of Radionuclides for Radiotracers in Nuclear Medicine,Thomas J. Ruth
3. Friesel, D. L. & Antaya, T. A., 2009. Medical Cyclotrons. Reviews of Accelerator Science and Technology, Volume 02, p. 133.
4. Review of Cyclotrons for the Production of Radioactive Isotopes for Medical and Industrial Applications
5. Milton, B. F., 1996. Commercial Compact Cyclotrons in the 90's. Cape Town, World Scientific Publishing Co.
6. Strijckmans, K., 2001. The isochronous cyclotron: principles and recent developments. Computerized Medical Imaging and Graphics, Volume 25, pp. 69-78.
7. Birattari, C. et al., 1987a. Biomedical applications of cyclotrons and review of commercially available models. Journal of Medical Engineering & Technology, 11(4), pp. 166-167.
8. IAEA, VIENNA, 2003 Manual for reactor produced radioisotopes
9. IAEA, 2006. IAEA-DCRP/2006. Directory of Cyclotrons used for Radionuclide Production in Member States 2006 Update. , Vienna: International Atomic Energy Agency.
10. Unparalleled contribution of technetium-99m to medicine over 5 decades. Eckelman WC. , JACC Cardiovasc Imag 2009;2:364–8.
11. Breaking America's dependence on imported molybdenum.Einstein AJ. , JACC Cardiovasc Imag 2009;2:369–71.
12. Perrier C, Segre E: Radioactive isotopes of element 43. Nature
13. Hansell, Cristina, 2008, "Nuclear Medicine's Double Hazard – Imperiled , Treatment and the Risk of Terrorism", Nonproliferation Review, Vol. 15, No.2.
14. Gould P. Medical isotope shortage reaches crisis level. Nature. 2009;460:312–313.
15. (Non-HEU Production Technologies for MOLYBDENUM-99 and TECHNETIUM-99m.
16. Report of the Expert Review Panel on Medical Isotope Production Presented to the Minister of Natural Resources Canada 30 November 2009
17. Van Noorden R. The Medical Testing Crisis. Nature 2013;504:2024.
18. OECD-NEA (2012) No. 7129, The Supply of Medical Radioisotopes: Market Impacts of Converting to Low-Enriched Uranium Targets for

Medical Isotope Production, OECD, Paris, France, ISBN 978-92-6499197-2.

19. OECD-NEA (2011) No. 6985, The Supply of Medical Radioisotopes: the Path to Reliability, OECD, Paris, France, ISBN 978-92-64-99164-4.

20. Frank N, HIPPEL V, LAURA H. Feasibility of eliminating the use of highly enriched uranium in the production of medical radioisotopes. Sci Global Secur 2006;14:151–62.

21. Beaver and Hupf, Production of 99mTc on a Medical Cyclotron: A Feasibility Study. J Nucl Med 1971;12:739–41

22. Report of the Expert Review Panel on Medical Isotope Production, Canada 30 November 2009.

23. Development of an automatic separation/extraction module for the accelerator 99mTc production from 100Mo enriched molybdenum metal targets(P. Martini1, A. Boschi1, L. Uccelli2, M. Pasquali1, G. Cicoria5,M. Marengo5, G. Lucconi5, M. Giganti1, G. Di Domenico3,G. Pupillo3, A. Taibi3, J. Esposito)

24. First in vivo imaging studies of cyclotron produced 99mTc-HMPAO (P. Martini3, A. Boschi3, L. Uccelli4, M. Pasquali3, A. Duatti3, G. Di Domenico5, G. Pupillo5, J. Esposito6, M. Loriggiola6,M. Giganti3, A. Taibi5, M. Gambaccini5, A. Salvini2, L. Strada2, M. Prata2, G. Cicoria7, M. Marengo7, G. Lucconi7, S. Manenti1,F. Groppi1, M. Bello6, N. Uzunov)

25. Lucconi, G. et al., 2014. Development of a solid target for cyclotron production of 99mTc. *Eur J Nucl Med Mol Imaging,* 41(Suppl 2), p. S347.

Bibliography

- Gagnon, K. et al., 2011. Cyclotron production of 99mTc: Experimental measurement of the 100 Mo(p,x)99Mo, 99mTc, and 99gTc excitation functions from 8 to 18 MeV. *Nuclear Medicine and Biology,* Volume 38, pp. 907-916.
- Hanemaayer, V. et al., 2014. Solid targets for 99mTc production on medical cyclotrons. *J Radioanal Nuc Chem,* Volume 1007-1011, p. 299.
- IAEA, 2008. *Cyclotron Produced Radionuclides: Principles and PracticeTechnical. Technical Reports Series No. 465,* Vienna: International Atomic Energy Agency.
- IAEA, 2009. *Cyclotron produced radio-nuclides: Physical Characteristics and production methods. IAEA Technical Report No. 468,* Vienna: International Atomic Energy Agency.
- Lucconi, G. et al., 2014. Development of a solid target for cyclotron production of 99mTc. *Eur J Nucl Med Mol Imaging,* 41(Suppl 2), p. S347.
- Qaim, S. M., 2004. Use of cyclotron in medicine. *Radiation Physics and Chemistry,* Volume 71, p. 917–926.
- Direct Production of ^{99m}Tc via ^{100}Mo(p,2n) on Small Medical Cyclotrons , Vancouver, British Columbia, Canada
- Incropera FP, Dewitt DP, Bergman TL and Lavine AS. Introduction to Heat Transfer. Fifth Edition. New York: John Wiley & Sons, 2007.
- SOLID TARGET SYSTEM FOR USE ON AN 11 MeV CYCLOTRON
- Andrew Carl Williamson University of Tennessee, Knoxville
- (GE MEDICAL SYSTEMS, 2004)
- Lucconi, G., Cicoria, G., Pancaldi, D. & Marengo, M., 2013. Assessment of the feasibility of producing 99mTc with a 16.5 MeV biomedical cyclotron using the TALYS nuclear reaction program and FLUKA code. *Clin Transl Imaging,* 1(Suppl 1), pp. S1S38.
- Qaim, S. M., 2004. Use of cyclotron in medicine. *Radiation Physics and Chemistry,* Volume 71, p. 917–926.

12. Acknowledgements

Completing this thesis, I feel deeply indebted to many people who have greatly inspired and supported me during my study at University of Bologna and the writing of this thesis.

First and foremost I wish to thank my coordinate Professor Domiziano Mostacci for his great encouragement, support and guidance of almost a year of development. I will never forget the warm hosting and amazing help since the first day I arrived in Bologna as a master student for an Erasmus exchange. Ever since that day I felt very welcome in your group.

A very special acknowledge goes to my co-advisor Dr. Mario Marengo. I really felt your enthusiasm about the project, your support and all the trust you put in me while letting me explore all kinds of ideas needed when creating new things. This year, studying and working in your lab, I learned technically and scientifically a lot. Without your supervision, I would not have completed this challenging project.

I would like to express my deepest gratitude to my promoter of National University of Athens, Professor Marios Anagnostakis for the opportunity he gave me to come and finish my studies at the University of Bologna and collaborate with great people. All this year his confidence, invaluable guidance and encouragement kept me focused when I sometimes hesitated to move forward because of difficulties I may faced. I'm really grateful for the trust and the responsibility you gave me.

I'm as well grateful to the opportunity I had to collaborate with the research stuff in Hospital St. Orsola-Malpighi and especially with Angelo, Sara, Federico and Giulia. All the days of working, the technical support in the lab, the guidance you offered to me not to mention the fun during the unofficial work discussion (coffee break) will be unforgettable. A very special thanks to Sara, she was always supportive and glad to help me like a real friend.

Last but not least, I own a huge gratitude and thanks to my family, my parents and my brothers for their love, patience and their dedication of many years of support during my undergraduate studies that provided the foundation for this work. I'm especially grateful to my parents who inculcated to me the thirst of knowledge and the importance of fighting for what you desire.

Anastasia
June 30th, 2015
Bologna, Italy

This page was intentionally left blank